Joint optimization of Beam Placement and Shaping for Multi-Beam High Throughput Satellite systems using Gradient Descent

by Rubén Alinque Dianez

May 2020

Bachelor's Final Thesis

Submitted to the faculties of

Facultat de Matemàtiques i Estadística (FME)
Escola Superior d'Enginyeria Industrial, Aeroespacial i Audiovisual de Terrassa (ESEIAAT)
of Universitat Politècnica de Catalunya (UPC) - BarcelonaTech

In partial fulfillment of the requirements for the

Bachelor's Degree in Aerospace Technology Engineering and **Bachelor's Degree in Mathematics**

Under the guidance of
Prof. Edward F. Crawley, MIT

Abstract

The satellite communications market is changing and new generation of satellites will have unprecedented levels of flexibility and scalability: future multi-beam High Throughput Satellites (HTS) are expected to be able to operate thousands of beams simultaneously, each with a set of fully-dynamic parameters to tune. This poses new challenges when it comes to efficiently managing the increasing amount of resources. Two of these challenges are linked to the beam placement (i.e., defining the pointing direction for each beam) and beam shape (i.e., optimizing the gain distribution among covered users) problems. Understanding how to exploit these two flexibilities could improve the efficiency, reducing the required RF power and enabling the accommodation of new users into the system. Thus, this Thesis focuses on the joint beam placement and shaping optimization.

Previous literature does not fully tackle the joint problem, it only focuses on solving each of them individually. This Thesis proposes two Gradient Descent-based algorithms to address the joint optimization of beam placement and shape and analyze their suitability under realistic scenarios. The considered scenarios differ in density of the user terminals to also study the effect of this variable on the performance of the algorithms. In order to carry out the simulations, a model of the O3b mPower constellation is used and the transmitter antenna is designed to have similar characteristics of those of MEO satellites. As a baseline, an heuristic approach to beam pointing is used; and a variant of this algorithm is considered as well when comparing the results. Each approach is measured on the provided gain to the user terminals, the number of beams used to achieve it, and the number of terminals that are left uncovered at the end of the optimization.

The results show that the joint optimization is more suited for denser scenarios. Depending on the situation of the satellite operator (for instance, if its set of customers tends to be sparse) simpler methods achieve good enough solutions. However, a big satellite operator providing service to thousands of customers in dense areas will benefit from it, achieving improvement in performance with the same (or even less) usage of resources. Additionally, one of the proposed formulations reduces the number of beams that have at least one uncovered user terminal from 20% to 0%.

Keywords: Beam placement, Beam shaping, High-Throughput Satellites, Multi-beam Satellite System, Satellite communications.

AMS Code: 90C29.

Resumen

El mercado de las comunicaciones por satélite está cambiando y la nueva generación de satélites tendrá niveles de flexibilidad y escalabilidad sin precedentes: se espera que los futuros Satélites de Alto Rendimiento de múltiples haces (HTS, por las siglas en inglés) puedan operar miles de haces simultáneamente, cada uno con un conjunto de parámtetros completamente dinámicos para sintonizar. Esto plantea nuevos desafíos cuando se trata de administrar eficientemente la creciente cantidad de recursos. Dos de estos desafíos están vinculados a: la ubicación del haz (es decir, definiendo la dirección para cada haz) y a la forma del haz (es decir, optimizando la distribución de ganancia entre los usuarios cubiertos). Comprender cómo explotar estas dos flexibilidades podría mejorar la eficiencia, reducir la potencia requerida y permitir el alojamiento de nuevos usuarios en el sistema. Por lo tanto, esta tesis se centra en la optimización conjunta de la posición y forma de los haces.

La literatura actual no aborda completamente el problema conjunto, solo se enfoca en resolver cada uno de ellos individualmente. Esta tesis propone dos algoritmos basados en el algoritmo de descenso del gradiente para abordar la optimización conjunta de la colocación y la forma del haz y analizar su idoneidad en escenarios realistas. Los escenarios considerados difieren en la densidad de los terminales, para también estudiar el efecto de esta variable en el rendimiento de los algoritmos. Para llevar a cabo las simulaciones se utiliza un modelo de la constelación O3b mPower y la antena del transmisor está diseñada para tener características similares a aquellas de los satélites MEO. Como referencia se utiliza un algoritmo heurístico de colocación de haces; y una variante de este algoritmo también se considera al comparar los resultados. Cada enfoque se mide según la ganancia proporcionada a los terminales, el número de haces utilizados para alcanzarlo y el número de terminales que quedan sin cubrir al final de la optimización.

Los resultados muestran que la optimización conjunta es más adecuada para escenarios más densos. Dependiendo de la situación del operador de satélite (por ejemplo, si su conjunto de clientes tiende a ser disperso), los métodos más simples logran soluciones suficientemente buenas. Sin embargo, un gran operador de satélites que brinde servicio a miles de clientes en áreas densas se beneficiará de ello, logrando una mejora en el rendimiento con el mismo (o incluso menos) uso de recursos. Además, una de las formulaciones propuestas reduce el número de haces con al menos un usuario no cubierto de un 20% a un 0%.

Palabras clave: Colocación de haces, Conformación de haces, Satélites de alto rendimiento, Sistema satelital multihaz, Comunicaciones satelitales.

Código AMS: 90C29.

Resum

El mercat de les comunicacions per satèl·lit està canviant i la nova generació de satèl·lits tindrà nivells de flexibilitat i escalabilitat sense precedents: s'espera que els futurs Satèl·lits d'Alt Rendiment de múltiples feixos (HTS, per les sigles en anglès) puguin operar milers de feixos simultàniament, cadascun amb un conjunt de paràmetres completament dinàmics per sintonitzar. Això planteja nous reptes quan es tracta d'administrar eficientment la creixent quantitat de recursos. Dos d'aquests reptes estan vinculats a: la ubicació del feix (és a dir, definint la direcció de cada feix) i la forma del feix (és a dir, optimitzant la distribució de guany entre els usuaris coberts). Comprendre com explotar aquestes dues flexibilitats podria millorar l'eficiència, reduïr la potència requerida i permetre l'allotjament de nous usuaris al sistema. Per tant, aquesta tesi es centra en l'optimització conjunta de la posició i forma dels feixos.

La literatura actual no aborda completament el problema conjunt, només s'enfoca en resoldre cada un d'ells individualment. Aquesta tesi proposa dos algorismes basats en l'algorisme de descens del gradient per abordar l'optimització conjunta de la col·locació i la forma de feix, i analitzar la seva idoneïtat en escenaris realistes. Els escenaris considerats difereixen en la densitat dels terminals, per també estudiar l'efecte d'aquesta variable en el rendiment dels algorismes. Per dur a terme les simulacions s'utilitza un model de la constel·lació O3b mPower i l'antena del transmissor està dissenyada per tenir característiques similars a aquelles dels satèl·lits MEO. Com a referència s'utilitza un algoritme heurístic de col·locació de feixos; i una variant d'aquest algorisme también es considera a l'hora de comparar els resultats. Cada solució es mesura segons el guany proporcionat als terminals, el nombre de feixos utilitzats per aconseguir-ho i el nombre de terminals que queden sense cobrir al final de l'optimització.

Els resultats mostren que l'optimització conjunta es més adequada per escenaris més densos. Depenent de la situació de l'operador de satèl·lit (per exemple, si el seu conjunt de clients tendeix a ser dispers), els mètodes més simples aconsegueixen solucions prou bones. No obstant això, un gran operador de satèl·lits que brindi servei a milers de clients en àrea denses es beneficiarà d'això, aconseguint una millora en el rendiment amb el mateix (o inclús menys) ús de recursos. A més, una de les formulacions proposades redueix el número de feixos amb algún usuari no cobert d'un 20% a un 0%.

Paraules clau: Col·locació de feixos, Conformació de feixos, Satèl·lits d'alt rendiment, Sistema satel·lital multifeix, Comunicacions satel·litals.

Codi AMS: 90C29.

Acknowledgements

First and foremost, I would like to thank Prof. Edward Crawley and Dr. Bruce Cameron for allowing me the opportunity to pursue this fulfilling experience at MIT. They have always been supportive and have given me invaluable guidance for the completion of this thesis. Ed, Bruce, it has been an honor to work with you.

Thank you to all the ESL laboratory for welcoming me, specially to the System Architecture Group: Damon, Iñigo, Markus, Nils, Juanjo, Skylar, and Sydney. Juanjo and Markus deserve a special mention for all the help and advice I received from them regarding both personal and professional endeavors.

I don't want to miss the chance to thank Prof. Miquel Sureda, professor at UPC, and Prof. Miguel Angel Barja, director of CFIS, without whom this project would not have been possible. Thank you for fulfilling my dream of studying at MIT.

I would like to thank Fundació Cellex for the financial support during the development of this thesis and my stay in Boston.

I would also like to thank SES S.A. for their support and the model used to recreate the test scenarios.

Last but definitely not least, I would like to thank my friends and family. They all have supported me and believed in me during all these years of undergraduate, even in times when I didn't. Without them, I would not be who I am and would not have achieved what I have achieved.

Per aspera ad astra.

Contents

CONTENTS

List of Figures

1. Introduction

This chapter aims to define the main guidelines of this Thesis. It starts giving context of the current state of the satellite communication market, and how it is growing over time, and motivating why it is interesting the joint optimization of beam placement and shape. After that, the two main research questions are stated, followed by the scope and delimitations of the project. The chapter ends presenting the structure of the remaining of the Thesis.

1.1. Context and Motivation

The satellite communications market is growing fast, and has changed significantly in the last 30 years [3] because of an increased demand of connectivity services to remote locations that do not have ground communications infrastructures [6], or to serve the mobility sector (airplanes and ships). In 2016, total revenues were $329M, and they are expected to be $1.1T in 2040 [7].

To deal with this rising demand, which is bursty by nature, satellite operators are moving towards more flexible satellites [8]. Recent designs are replacing analogue payloads with digital communication ones, which will allow for more flexible resource allocation [7]. Figure 1.1 shows the main changes in terms of flexibility between present and future satellite systems.

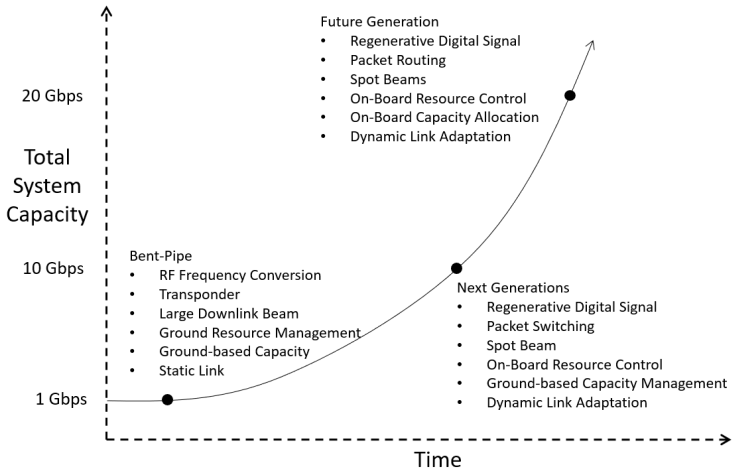

Figure 1.1: Generational Changes in Satellite Systems. Source: [1]

One current trend in space industry is the use of high-throughput multi-beam constellations. We will have, for instance, large LEO constellations such as SpaceX's [9], Telesat's [10], or OneWeb's [11]. They consist of hundreds or thousands of multi-beam satellites with the capacity for producing tens or hundreds of spot beams each. In MEO and GEO orbits, Viasat-3 [12] is a trio of satellites with a capacity of 92 beams each, and O3b mPower [13] is a group of seven satellites, each with capacity of producing thousands of beams. All these new generation payloads need to be flexible to be able to adapt to the demand changes [14].

With flexible payloads, myriads of degrees of freedom appear that cannot be managed using traditional methods. In [15], four main flexibilities are identified:

- **Power adjustment**: setting the transmitted radio-frequency (RF) power per carrier.
- **Frequency assignment**: setting the coloring scheme and spectrum allocation within the carriers.
- **Beam pointing**: determining the pointing / steering direction of each beam.
- **Beam shaping**: defining the shape (i.e., narrowing or widening) of each beam.

Another current trend, already introduced, is providing global connectivity services. In [16], it is concluded that MEO and GEO constellations are the most cost-effective in providing connectivity to uncovered or under-served regions. It is also stated that, for these space systems, the number of satellites and beams play a major role to achieve the optimum cost-efficiency.

With this in mind, beam pointing and beam shaping are problems that the satellite operators need to solve in order to build the most cost-efficient architectures, as both are needed to define the set of beams of the system.

1.2. Research questions

The main goal of this Thesis is to understand the achievable beams' configurations by optimizing both the pointing direction and shape, and explore the tradeoffs between performance and usage of resources. In particular, the main research question that this Thesis tries to answer is:

Research question 1

What is the value of the joint optimization of beam placement and shaping for multi-beam satellite constellations?

Additionally, as the approach uses the gradient descent technique, which has not been used in this context (as it is explained in Chapter 2), this Thesis aims to determine if it is a good optimization method to apply:

Research question 2

In the context of gain optimization for multi-beam satellite constellations, is gradient descent a suitable optimization method?

1.3. Scope and Delimitations

What this Thesis intends to accomplish:

- Provide a summary of satellite communications systems theory related to the problems being solved, beam placement and beam shape.
- Propose formulations to tackle the joint problem and analyze them.
- Use test cases to test the performance of such formulations.
- Propose future work in this topic and possible improvements.

What this Thesis does not intend to accomplish:

- Provide a summary of the theory behind beamforming and phased arrays in general.
- Propose a solution that takes into account the demand of the user terminals.
- Design an algorithm subject to a particular time constraint.

1.4. Thesis structure

The remainder of the Thesis is as follows:

Chapter 2 presents the current state of literature regarding the problem and the research objectives. Chapter 3 gives the theoretical background of satellite communications systems needed to follow this Thesis, giving emphasis to the description of the gain distribution within a beam and its role in a link budget. Chapter 4 is the problem formulation, where the beam placement and beam shape problems are explained individually, the joint problem is defined, and formulations are proposed to tackle it. Chapter 5 goes through the modeling for the problem, from the model of the constellation that is used to the modeling of the gain distribution as a function of the pointing and shape of the beam. Chapter 6 is the methodology used along this Thesis. The algorithms, how Gradient Descent can be used for this problem, the metrics, and the test cases are presented. Chapter 7 presents the obtained results. Finally, Chapter 8 summarizes the main findings and addresses the research questions of the Thesis.

2. Literature review

This chapter aims to present the state of the art of similar problems than those this Thesis aims to solve. It starts elaborating on current methods to define the pointing direction and shape of a beam, respectively. Then, some optimization techniques, along with metrics used, are discussed. With this information, it follows a summary of literature that comprises all the knowledge in these particular areas, which leads to the research opportunities of the Thesis. The chapter ends with the definition of the specific objectives of the Thesis.

2.1. Beam placement

Choi [17–20] has made several contributions. In [18] and [17] he argues that, by optimizing the deisgn of multi-beam pattern of antennas, the efficiency of transmission and power management can be improved. Additionally, increasing the number of beam entails a significant enhancement in spectral efficiency. In [19], his work focuses on scheduling for phased arrays. The real-time algorithm performs several tasks, being power allocation and antenna gain pattern design among them. He shows that, for random traffic, it can be achieved up to 94 % of the analytical result. In a follow-up article, [20], he studies phased arrays with multiple beam antennas and concludes that better performance, especially in dense areas, can be achieved by more flexible power allocation.

Jahn [21] solves the resource allocation problem of beam placement and frequency planning by using graph theory algorithms. In particular, he tackles the problem of beam placement (considering beams of fixed shape) as a clique cover problem.

Camino [22, 23] uses a greedy approach [23] and a mixed-integer linear programming method [22] to optimize the integrated design of satellite payload. The problem consists in defining a set of beams (each with its own size) to cover an area of non-uniform traffic. The aim is to optimize the load balancing. The conclusion is that, for smaller scenarios, the mixed-integer linear programming outperforms the greedy algorithm, while for larger cases is the opposite. In a later work, [24], he studies the application of mixed-integer linear programming to the beam placement problem by linearizing the constraints that

depend on the Euclidean norm, which are common in this problem. The aim is to minimize the distance of every terminal to the center of its beam.

Pachler [4] proposes an algorithm to solve two subproblems of the resource allocation problem for multi-beam satellites in large LEO constellations: static beam placement and static frequency plan. With respect to beam placement, it is a fast approximation to the solution using graph theory. It later uses the result of the beam placement as constraints for the frequency assignment problem.

2.2. Beam shape

Qian [25] aims to balance the load between beams by dynamic beam coverage adjustments. The considered scenario is a heavy-loaded center beam with six surrounding beams. The results show that system throughput can be increased by dynamically switching between two sets: one with a wider center beam and other with a narrower center beam.

Schubert and Boche [26] derive an analytical framework for the joint power and beamforming optimization for downlink communication links. They use two objectives to optimize for: the maximization of the achievable signal-to-interference-plus-noise ratio (SINR), and the minimization of the consumed power. They use an iterative algorithm which is proven to achieve the global optimum.

Kyrgiazos [27] tackles the joint problem of spectrum allocation and beam size adjustment. In particular, two different beam shapes are considered. The results show that, by using beams of different size, the total throughput can be improved by 11% compared to the scenario where all the beams are of equal size.

Sharma [28] studied the joint carrier allocation and beamforming for feeder links in Ka-band. The aim was to minimize the output energy. The results show that, combining the allocations, the system thorughput can be improved, compared to allocating them individually.

2.3. Optimization techniques

Jahn [21], Kyrgiazos [27], and Pachler [4] use graph theory as the optimization technique in their research. In particular, all three end up translating the problem into a clique cover problem. On the other side, Camino [22] and Choi [17–19] use mathematical programming: Lagrange multipliers the former, and Mixed-integer programming the latter. Camino [23], Qian [25], Wenqian [29], Schubert and Boche [26], and Sharma [28] use ad-hoc tehcniques, such as greedy algorithms.

Akbarzadeh [30] uses gradient descent to optimize the sensor placement to cover a given area. The metric, coverage, is treated as continuous and differentiable with the use of the sigmoid function, allowing the definition of an analytical, continuous, and differentiable function able to be solved by using gradient descent.

2.4. Summary of literature and research opportunities

A summary of the literature is shown in Table 2.1, along with the proposed contribution of this work. The table uses a three-color scale: red means that it has not been considered or used (the former in the case of a dynamic parameter, the latter for a optimization technique), yellow means that it has been partially considered/used, and green that it has been considered/used.

In general, we observe little correlation between the dynamic parameter considered and the optimization technique used. We see that we can tackle beam placement using graph theory but also mathematical programming. In beam shape it is more clear: most of the options fall into miscellaneous / ad-hoc approaches.

Additionally, little work towards the fully consideration of both placement and shape is observed.

With this in mind, we formulate two main literature gaps:

- **Gap in the fully consideration of both beam placement and beam shape**. Beam placement and beam shape are two naturally-coupled problems, as, for instance, to define the pointing direction of a beam one has to account for the shape to cover all the user terminals. However, little work has been done to consider the joint optimization of these two parameters. The successful optimization of both flexibilities is likely to provide operators competitive advantage.

- **Gap in optimization techniques to consider beam shape**. For this parameter, the approaches tend to be ad-hoc, as previously mentioned. There are many different ways to model the shape of a beam, thus leading researchers to apply different optimization techniques. Setting a framework to optimize both parameters will help the study of the interaction and natural tradeoffs between them.

		Dynamic param. considered				Optimization technique			
		Power	Frequency plan	Beam Placement	Beam Shape	Gradient Descent	Math. Prog.	Graph Theory	Ad-hoc
Beam placement	Choi [17–19]								
	Jahn [21]								
	Camino [22], [23], [24]								
	Pachler [4]								
Beam shape	Qian [25]								
	Wenqian [29]								
	Schubert, Boche [26]								
	Kyrgiazos [27]								
	Sharma [28]								
	Proposed Alinque								

Legend: Fully considered | Partially considered | Not considered

Table 2.1: Summary of the literature review based on dynamic parameters considered and optimization techniques used. The proposed contribution is included in the last row.

2.5. Specific objectives

This chapter defines the specific objectives based on the reviewed literature. This Thesis aims to contribute to the identified gaps and develop a methodology to solve the coupled beam placement and shaping problem for multi-beam satellite systems. This is done using Gradient Descent.

The specific objectives can be formalized with the following to-by-using statement:

The specific objective of this Thesis is:

To *optimize the joint beam placement and shaping problem in a multi-beam satellite system maximizing the gain attained,*

by *modeling the gain distribution of the transmitter antenna and finding the best pointing direction and shape for each beam,*

using *Gradient Descent.*

3. Satellite communications systems

The aim of this chapter is to explain the main theoretical concepts behind satellite communications systems, giving the reader an holistic view and background of the basis of this Thesis. If the reader is interested in deeper or more advanced explanations, please refer to [3].

3.1. Configuration of a satellite communication system

Figure 3.1 illustrates an overview of the configuration of a satellite communication system. It consists of a space segment, a control segment, and a ground/user segment. The first one is a set of one or several satellites organised into a constellation, the control segment consists of the ground facilities for the control and monitoring of the satellites, the traffic, and on-board resources, and the ground segment are all the earth stations.

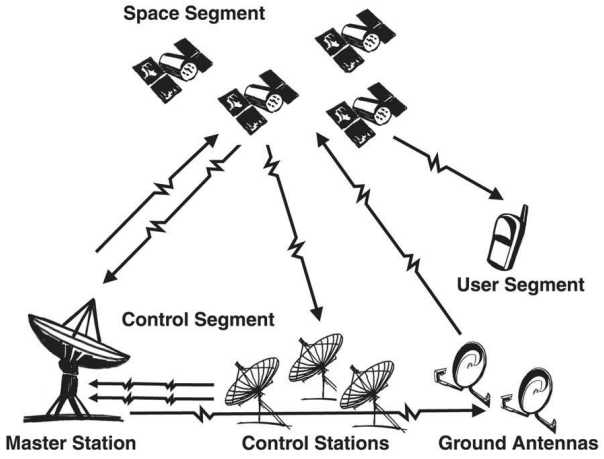

Figure 3.1: Overview of the configuration of a satellite communications system. Source: [2]

3.1.1. Communication links

The types of links are shown in Figure 3.1, and are:

- the uplinks, from the earth stations to the satellites.
- the downlinks, from the satellites to the earth stations.
- the intersatellite, between the satellites.

Uplinks and downlinks consist of radio frequency modulated carriers, while intersatellite links can be either radio frequency or optical.

One parameter of importance for the design of a link is the bandwidth, B, occupied by the carrier. For satellite links, the trade-off between required carrier power and occupied bandwidth is paramount to the cost-effective design of the link.

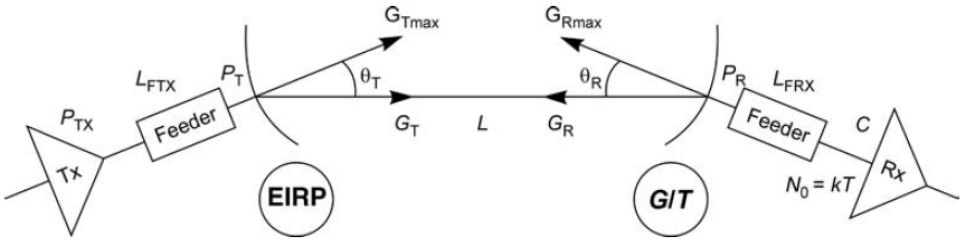

Figure 3.2: Configuration of a link. Source: [3]

Figure 3.2 represents the elements participating in a link. On one side, the transmit equipment consists of transmitter Tx connected to the transmit antenna. The transmitter antenna has gain G_T in the direction of the receiver. P_T is the power transmitted in the direction of the receiving equipment. On the other side, the receiving equipment is made of the receive antenna (this one has gain G_R in the direction of the transmit equipment), connected to the receiver Rx. From the transmitter to the receiver, one has to take into account that there is a path loss L.

3.2. Antenna parameters

The antenna design is paramount to the performance of the communication links. The following sections present the most important parameters to consider while defining these devices.

3.2.1. Gain

The gain of an antenna is the ratio of the power produced by the antenna from a far-field source on the antenna's beam axis to the power produced by a hypothetical lossless isotropic antenna. The gain is maximum in the direction of maximum radiation (also called the boresight) and has a value given by:

$$G_{max} = \eta(\pi D/\lambda)^2 = \eta(\pi Df/c)^2 \tag{3.2.1}$$

Where η is the efficiency of the antenna, D the diameter of the reflector (we are assume circular aperture), and $\lambda = c/f$ (c is the speed of light, f is the frequency of the wave). Expressed in dBi (the gain relative to an isotropic antenna), the actual maximum antenna gain is:

$$G_{max,dBi} = 10 \cdot log_{10}[\eta(\pi D/\lambda)^2] = 10 \cdot log_{10}[\eta(\pi Df/c)^2] \tag{3.2.2}$$

3.2.2. Radiation pattern and angular beamwidth

The previous definition of gain considers the gain in the steering direction of the antenna. The radiation pattern illustrates the variation of gain with respect to the direction. This pattern can be represented using a polar coordinate form (Figure 3.3a) or a cartesian coordinate form (Figure 3.3b). There is a main lobe, which contains the directions of maximum gain. There are also side lobes, which can be understood as unwanted radiation towards unwanted directions, and can affect the noise taken by other receivers.

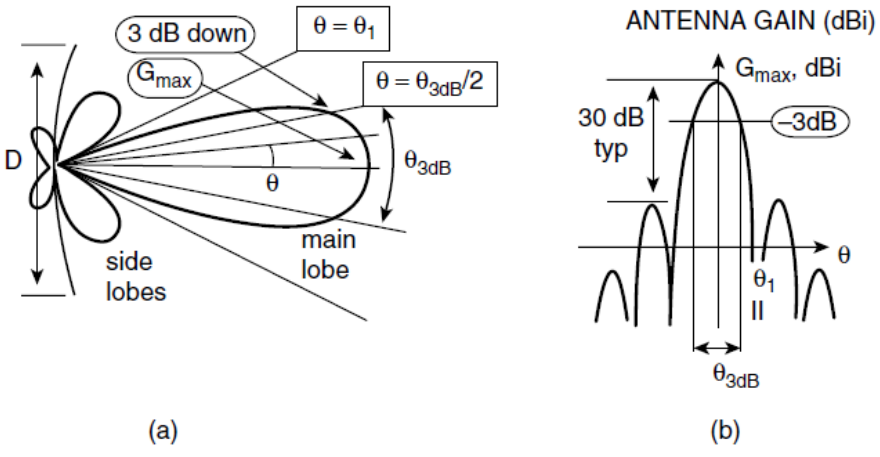

Figure 3.3: Antenna radiation pattern: (a) polar representation and (b) cartesian representation. Source: [3]

The angular beamwidth is the angle between the directions for which the gain corresponds to a given fallout with respect to the maximum. The 3 dB beamwidth is often used, which

corresponds to the angle between the directions in which the gain falls 3 dB with respect to the gain at boresight. This beamwidth is related to the ratio λ/D by a coefficient, for which a typical value of 70º is used, and leads to the expression:

$$\theta_{3dB} = 70(\lambda/D) = 70(\frac{c}{fD}) \quad [\text{deg}] \tag{3.2.3}$$

In a direction θ (with respect to the direction of maximum gain), the value of gain is:

$$G(\theta)_{dBi} = G_{max,dBi} - 12(\theta/\theta_{3dB})^2 \tag{3.2.4}$$

This expression is valid only for $|\theta| \in [0,\ \theta_{3dB}/2]$.

Combining equations 3.2.1 and 3.2.3, it can be seen that G_{max} depends on θ_{3dB} (in degrees) and does not depend on the frequency:

$$G_{max} = \eta(\pi Df/c)^2 = \eta(\pi 70/\theta_{3dB})^2 \tag{3.2.5}$$

In particular, from Equation 3.2.5 one can see that wider beams have less maximum gain, and viceversa.

3.2.3. Polarisation

The wave radiated by an antenna is composed of two orthogonal components: an electric field and a magnetic field. By convention, the direction of the electric field is known as the polarisation.

An antenna designed to transmit or receive a wave of given polarisation can neither transmit nor receive in the orthogonal polarisation. This allows the antenna to, between two same places, establish two simultaneous links with the same frequency.

3.3. Radiated power

With the radiation pattern defined, one can compute the radiated power of an antenna. To do so, it is interesting to consider two different metrics: the Effective isotropic radiated power, and the Power flux density.

3.3.1. Effective isotropic radiated power (EIRP)

The power radiated per unit solid angle by an isotropic antenna fed from source of power P_T is given by:

$$P_T/4\pi \quad [\text{W/steradian}] \tag{3.3.1}$$

If the transmission gain is G_T towards the direction of the antenna, it radiates a power per unit solid angle equal to:

$$G_T P_T/4\pi \quad [\text{W/steradian}] \tag{3.3.2}$$

The term $P_T G_T$ is called the *effective isotropic radiated power* (EIRP).

3.3.2. Power flux density

In a distance R from the transmitting antenna, if there is a surface with area A, it subtends a solid angle A/R^2. Then, with the previous section we can compute the power it receives:

$$P_R = (P_T G_T/4\pi)(A/R^2) = \Phi A \quad [\text{W}] \tag{3.3.3}$$

Φ is called the power flux density [W/m^2].

3.4. Received signal power

However, the power received from the transmitter gets affected by some losses, such as the free space loss. The following sections elaborate on the power captured by the receiver, accounting for losses.

3.4.1. Power captured by the receiving antenna and free space loss

As shown in Figure 3.4, a receiving antenna of effective aperture area A_{Reff} located at a distance R from the transmitting antenna receives power equal to:

$$P_R = \Phi A_{Reff} = (P_T G_T/4\pi R^2) A_{Reff} \quad [\text{W}] \tag{3.4.1}$$

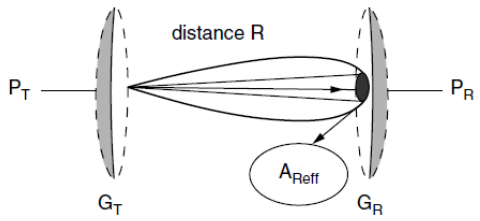

Figure 3.4: The power received by a receiving antenna. Source: [3]

A_{Reff} can be expressed as a function of the receiving gain (G_R):

$$A_{Reff} = G_R/(4\pi/\lambda^2) \quad [\text{m}^2] \tag{3.4.2}$$

Then, an expression for the received power:

$$\begin{aligned} P_R &= (P_T G_T / 4\pi R^2)(\lambda^2 / 4\pi) G_R \\ &= (P_T G_T)(1/L_{FS}) G_R \quad [\text{W}] \end{aligned} \tag{3.4.3}$$

Where $L_{FS} = (4\pi R/\lambda)^2$ is called the free space loss and represents the ratio of the received and transmitted powers in a link between two isotropic antennas. It is important to notice the square dependency with respect to the distance between the antennas, because it means that, for instance, for MEO and GEO constellations this loss is significantly more important than for LEO.

3.4.2. Additional losses

Due to system imperfections, in practice it is necessary to consider additional losses:

- Attenuation of waves as they propagate through the atmosphere, L_A. This one and the free-space loss make the Path Loss (L_P).
- Losses in the transmitting and receiving equipment, L_{TX} and L_{RX} respectively.
- Depointing losses, due to the antennas not being perfectly aligned. The value of this one can be extracted from Equation 3.2.4:

  $$L = 12 \left(\frac{\theta}{\theta_{3dB}} \right)^2 \quad [\text{dB}] \tag{3.4.4}$$

  We have one for each antenna.
- Polarisation mismatch losses. This can happen if the receiving antenna is not correctly oriented with respect to the polarization of the field (L_{POL}).

3.5. Noise

An antenna has to be able to identify the signal of interest within the received wave. In order to do that, the power of that signal has to be significantly greater than the power received by unwanted sources, which are considered noise. As we have already explored all the nuances with respect to the received power, the following sections elaborate on the noise and its characterization.

3.5.1. Origins of noise

Noise consists of all contributions whose power adds to the wanted carrier power from unwanted sources.

The origins of noise are:

- Sources of radiation located close to the receiving antenna. Also known as Thermal noise.
- Noise generated by the receiving equipment.

There is also noise coming from transmitters (others than the one that you wish to receive the signal from). This noise is described as interference.

3.5.2. Noise characterisation

A popular noise model is white noise, for which the power spectral density N_0 (W/Hz) is constant (Figure 3.5).

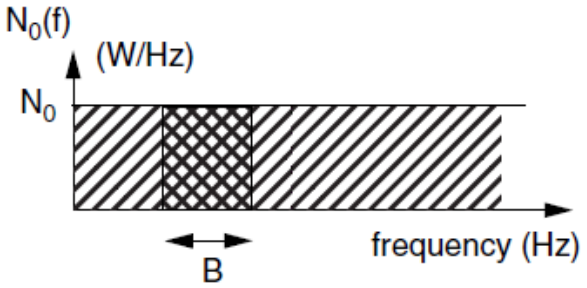

Figure 3.5: Spectral density of white noise. Source: [3]

The noise power N (W) captured by the receiving antenna with bandwidth B, is:

$$N = N_0 B \quad [\text{W}] \tag{3.5.1}$$

Real noise sources are not always similar to white noise, but the model is useful to represent the actual noise over a particular bandwidth.

The noise temperature of a noise source delivering a noise power spectral density N_0 is given by:

$$T = N_0/k \quad [\text{K}] \tag{3.5.2}$$

where k is Boltzmann's constant (= 1.379 x 10^{-23} $\frac{m^2 kg}{s^2 K}$ = -228.6 $\frac{dBW}{HzK}$). T represents the thermodynamic temperature of a resistance that produces the same noise power.

3.6. Individual link performance

With the characterization of both the received power and noise, one can measure the performance of the link. This is evaluated as the ratio of the received carrier power, C (P_R), to the noise power spectral density, N_0, and is quoted as the C/N_0 ratio, expressed in Hz.

On one side, from Chapter 3.4, the received carrier power is:

$$C = P_T + G_T + G_R - L_{FS} - L_A - L_{TX} - L_{RX} - LT - L_R - L_{POL} \quad [dB] \tag{3.6.1}$$

On the other side, from Chapter 3.5 (Equation 3.5.2), the noise power spectral density is:

$$N_0 = kT \quad [\text{W/Hz}] \tag{3.6.2}$$

Thus, the C/N_0 ratio is:

$$\frac{C}{N_0} = \frac{\frac{P_T G_T}{L_{TX} L_T} \frac{1}{L_{FPS} L_A} \frac{G_R}{L_R L_{RX} L_{POL}}}{kT} \tag{3.6.3}$$

3.7. Link performance with multi-beam antennas

From the previous sections, one can see that link performance depends on the gain of the transmitting antenna. From Equation 3.2.5, it can be seen that this gain is bounded by its beamwidth, θ_{3dB}. So, is constrained by the angular width of the beam covering the serving zone. If the service zone is covered using a single antenna beam, this is referred to as *single beam coverage*. Single beam antenna coverage follows one of these two alternatives:

- The satellite covers the whole region visible from the satellite (global coverage), allowing the establishment of long-distance links. In this case, the beamwidth value is high and the gain of the antenna becomes small.

- The satellite only covers part of the region by means of a spot beam, with smaller 3dB beamwidth. This benefits from a higher antenna gain, but the satellite cannot serve earth stations outside this narrow coverage. The earth stations that fall out of the coverage can only be reached by other methods, such as terrestrial links or other satellites (using intersatellite links).

Then, one needs to choose between extended coverage (serving with reduced quality to spread earth stations), or reduced coverage (providing better quality service to concentrated earth stations).

Multi-beam antenna coverage is a solution to consider these two alternatives. Satellite extended coverage can be produced by the union of several narrow beam coverages, each one of the beams with a high antenna gain due to its low beamwidth. The higher the number of beams, the better the link performance. Figure 3.6 shows the differences between the scenarios of global coverage and coverage by spot beams.

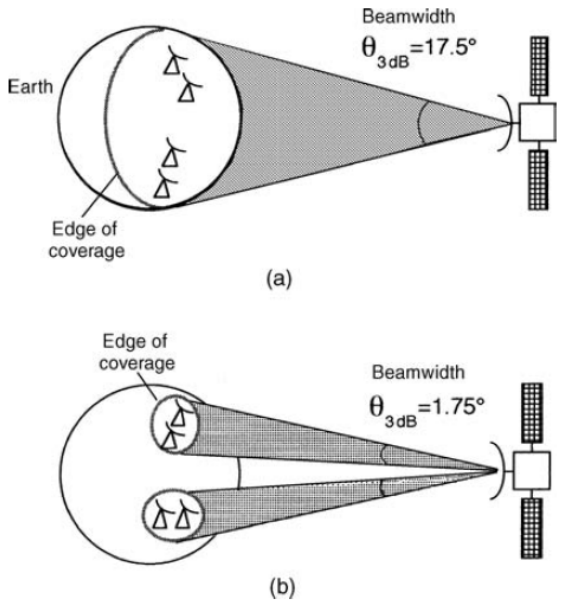

Figure 3.6: (a) Global coverage and (b) coverage by several narrow beams. Source: [3]

One major advantage of these systems is that it reduces $(\text{EIRP})_{station}$ and $(\text{G/T})_{station}$, which means a reduction in size (and cost) of the earth segment. This can be seen in Equation 3.6.3: for the same link performance, having a greater gain from the spot beams, allows the mentioned values to be smaller, hence reducing the size of the antenna at the ground station.

Another advantage of multibeam systems has to do with the frequency re-use. This consists of using the same frequency band several times to increase the total capacity of the network without increasing the allocated bandwidth.

One direct disadvantage of these systems, considering the last point, is the interference between beams. As illustrated in Figure 3.7, both in the uplink and downlink there appear problems with respect to the frequency domains of every beam, which becomes more complex to manage the more beams the system has.

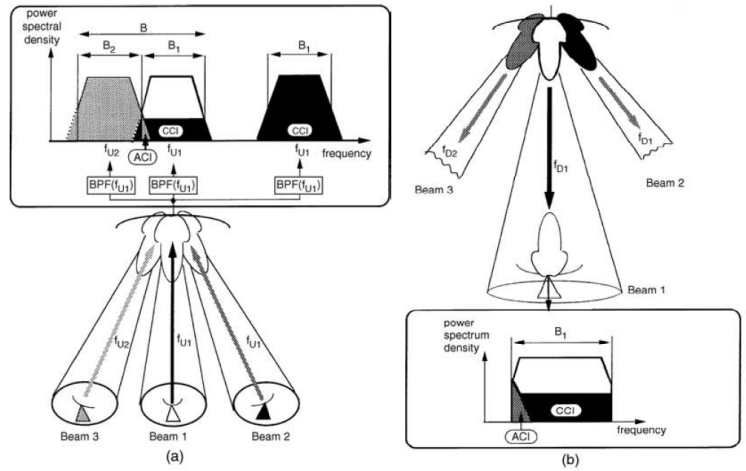

Figure 3.7: Self-interference between beams in a multibeam satellite system: (a) uplink and (b) downlink. Source: [3]

Another disadvantage has to do with the interconnection between covered areas. A multibeam satellite payload must be able to connect all earth stations and, consequently, provide interconnection of coverage areas. This payload, then, becomes more complex than that of a single beam satellite. In order to accomplish this, different techniques depending on the on-board processing capability need to be considered.

4. Problem formulation

This section aims to formulate the problem of joint beam placement and shaping optimization for a multi-beam satellite system. After the definitions, the problems of beam placement and beam shaping are explained separately, to understand both of them and their nuances. The last section covers the formulations for the joint problem.

4.1. Definitions

A user terminal, u, is defined by its location, $u = \{\text{lat: } \phi_q, \text{lon: } \theta_q\}$. $\mathcal{U}$ is the set of terminals, $\mathcal{U} = \{u_i\}$.

A beam b is defined by its location[1] and shape[2], $b = \{\text{lat: } \phi_b, \text{lon: } \theta_b, \text{k: } k_b\}$. Using Equations 3.2.3 and 5.3.3, equivalently one can use $\theta_{3dB,k}$ as a parameter for the shape. $\mathcal{B}$ represents a set of beams, $\mathcal{B} = \{b_i\}$.

At any time, each beam has an assigned satellite S uniquely defined[3]. Its position can be referred to as $\vec{r}_s(t)$ or S(t).

4.2. Beam placement

The beam placement problem, or beam pointing problem, consists in defining a set of beams and a mapping between this set and the set of terminals. The constraints and metrics related to this problem can defer, but in this Thesis the aim is to minimize the

[1] The location of the center of the beam projected into the Earth.

[2] Only circular beams are considered within this Thesis. Thus, only one parameter is enough to define the shape.

[3] The process of assigning a satellite to a beam for a given time is called link routing, and is outside the scope of this Thesis. In [16] it is mentioned the routing strategy used in this Thesis, that was not developed by the author.

amount of resources (the number of beams, $|\mathcal{B}|$, is used as a proxy) while ensuring that every user terminal is covered by some beam. So, the objective is to cover all the users with the minimum number of beams.

The inputs are the set of user terminals, $\mathcal{U}$, and a given shape. The shape can be represented by its beamwidth angle, θ_{3dB}. On the other side, the outputs are both the set of beams, $\mathcal{B}$, and the mapping BP:

$$\begin{array}{rccc} BP: & \mathcal{U} & & \mathcal{B} \\ & u & \longmapsto & BP(u) = b \end{array}$$

As the beam shape is fixed in this problem, defining the set of beams is essentially setting the locations (ϕ_b and θ_b).

For BP to be feasible, if we have a user terminal u, whose location is U, its beam center location is B, and the satellite's position is S(t), the following condition needs to be fulfilled:

$$\angle(\overrightarrow{SU}, \overrightarrow{SB})(t) \leq \theta_{3dB}/2 \quad \forall t \tag{4.2.1}$$

In other words, each user terminal $u \in \mathcal{U}$ needs to be inside the footprint of BP(u) at any given time.

Note that BP is not necessarily injective, as two different users can be mapped to the same beam (BP(u_1) = BP(u_2) $\nRightarrow$ $u_1 = u_2$). However, BP should be surjective, as having a beam without any user mapped to it would not make sense in this context.

It is also important that one user u can fulfill Equation 4.2.1 considering a beam b different from BP(u). This only means that u is inside the footprint of b, but it is not necessarily linked to it.

In terms of constraints, the main one is that each user has to be mapped to one and only one beam. So, there should not be any ambiguity when one states BP(u).

The problem formulation would be, then, if χ is the set of feasible mappings that cover all the terminals, and $\mathcal{B}_\chi$ the associated sets of beams (image of the mapping):

$$\begin{array}{l} min. \quad |\mathcal{B}_x| \\ x \in \chi \end{array}$$

4.3. Beam shape

The beam shaping problem consists in computing, for each beam of a multi-beam system, the optimum shape to provide a better performance. In this Thesis, the average (in time)

gain attained by the terminals is the objective function to maximize:

$$\bar{\mathcal{G}}_{\text{total}} = \sum_{b \in \mathcal{B}} \bar{\mathcal{G}}_b$$

$$\bar{\mathcal{G}}_b = \sum_{u \in \mathcal{U}_b} G(\bar{b}, u)$$

Being $\mathcal{U}_b \subset \mathcal{U}$ the set of terminals linked to beam b, and $\bar{G}(b,u)$ the average gain provided to u by beam b.

As the locations of the beams are fixed in this problem, the variables are the shape parameters, k_i of the beams.

The input, thus, is the outcome of a placement: a set of beams, $\mathcal{B}$, the set of user terminals, $\mathcal{U}$, and a mapping BP. The outcome is another set of beams $\mathcal{B}'$ with the same locations as the beams in $\mathcal{B}$ but different shapes (equivalently, different $\theta_{3dB,b}$).

Note that, in $\mathcal{B}'$, each beam has its own shape.

4.4. Joint beam placement and shaping

The joint problem consists in defining a set of beams to cover the user terminals in the most efficient way. The input is just the set of user terminals $\mathcal{U}$. And the outcomes are both a set of beams, $\mathcal{B}$, and a mapping of the placement, BP.

The trickiest part of the problem is to define *the most efficient way*. Let's discuss two completely different scenarios and their nuances to give a glance on why that definition is not obvious:

- Suppose that one wants to **maximize the provided gain to users**. Then, the utopia point would be to set a beam completely centered on each of the user terminals. All users are receiving the maximum possible gain, as they have no depointing loss (see Chapter 3.4.2). The most obvious drawback is that maintaining all those beams would require a high amount of power and would significantly produce interference. Additionally, another foreseeable shortcoming is that the frequency plan would give small bandwidths to the beams to avoid that interference, which also affects power. As a satellite has an available spectrum, having more beams implies making more (and, thus, smaller) subdivisions of it.

- Suppose, now, that one decides to keep the philosophy behind the beam placement problem and tries to **minimize the number of beams**. In that case, the main shortcoming is that the gain distribution would be subpar. Having a low number of beams implies, on average, having more users per beam, which means having terminals near the contour of the beam. The depointing loss would be significant.

One purpose of this Thesis is to explore the trade-off between these two main metrics: Gain and number of beams; representing, respectively, *how good or bad is our service* and *how much power do we need to deploy the system.*

The expected trade-off, qualitatively, can be seen in Figure 4.1:

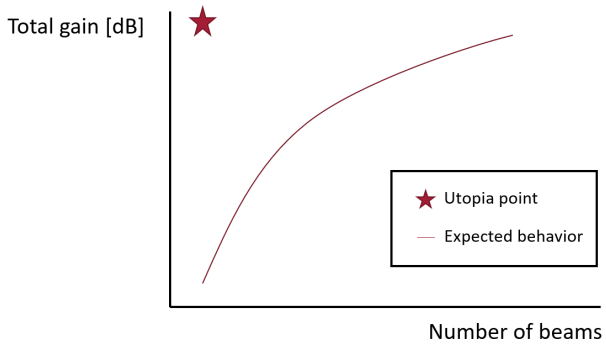

Figure 4.1: Trade-off between Gain and Number of beams. A star represents utopia point: maximum gain with minimum number of beams.

With this in mind, this Thesis proposes two formulations for the problem: a **local** formulation and a **global** formulation. They correspond to different hypothetical business situations. The first one consists in a fine-tuning of the outcome of the beam placement problem, where we optimize both pointing and shape maintaining the mapping BP. It is meant to be useful for operators in the middle of a service, where the linking of users to beams might not be able to change for some reasons. The latter, on the other side, optimize for the same parameters but without being constrained by any mapping. Thus, the mapping will be part of the outcome of the global formulation. This can be useful to setup a whole new service, where all the possibilities of linking users to beams are open.

4.5. Local formulation

The rationale behind this formulation is to improve a given placement. As, to generate a placement, one does not need to consider the gain distribution, the aim of this formulation is to take such placement and fine-tune it. The formulation itself is the same as in the beam shape problem, Chapter 4.3, with one important caveat.

While the objective function is the same - the aim is to maximize the provided gain - , the locations of the beams become variables of the optimization process. In other words, $\mathcal{G}_b$ is no longer a function of k only, but of the location of the beam as well.
Then, the objective function is:

$$\mathcal{G}_{\text{total}} = \sum_{b \in \mathcal{B}} \bar{\mathcal{G}}_b$$

With the understanding that now $\mathcal{G}_b = \mathcal{G}_b(\phi_b, \theta_b, k_b)$, and $\bar{\mathcal{G}}_b$ is the averaging in time of $\mathcal{G}_b$.

The input, then, is the set of user terminals $\mathcal{U}$, a set of beams $\mathcal{B}$, and a placement BP. The outcome, on the other side, is another set of beams $\mathcal{B}'$ with the same cardinality as $\mathcal{B}$ but, potentially, different shapes and locations.

As it is described in Chapter 6.4.1, the input for this formulation is the outcome of the beam placement problem, to exploit and try to get the maximum gain from a placement that uses the minimum number of beams possible.

4.6. Global formulation

To goal of the global formulation is to find the global optimum in terms of provided gain considering all beams simultaneously.

The local formulation optimizes $\mathcal{G}_b$ for each beam, and each function is completely independent from the others, as they consider different subsets of terminals. The global formulation, thus, intends to have a unique function that considers the whole set of terminals and beams.

The input is the set of user terminals $\mathcal{U}$ and a set of beams $\mathcal{B}$. The output is another set of beams, $\mathcal{B}'$, and a beam placement BP.

The objective function is:

$$\mathcal{G}(\mathcal{B}) = \sum_{b \in \mathcal{B}} \sum_{u \in \mathcal{U}} \bar{G}(b, u) X_{b,u} \tag{4.6.1}$$

Where $X_{b,u}$ is a binary variable:

$$X_{b,u} = \begin{cases} 1 & \text{if user } u \text{ is linked to beam } b \\ 0 & \text{otherwise} \end{cases}$$

One can understand the formula as *sum the provided gain to a user if a beam is covering the user and is the only one doing so.* These terms are to avoid the possible overlapping of beams. In practice, Equation 4.6.1 is not used as shown, as it is explained in Chapter 6.4.2. The main reason is to avoid the binary terms to be able to apply the Gradient Descent algorithm. Thus, the overlapping is considered in a different way.

A natural constraint is that, at the end, all the users need to be covered by some beam. In Chapter 6.4.2, it is shown how to guarantee this fact.

5. Model description

This chapters aims to describe the model used in the simulations. The objective is to give an understanding of the different entities that play a role in the problem formulation presented in Chapter 4.

5.1. mPower Constellation

As already introduced in Chapter 1.1, O3b mPower is a MEO constellation consisting of seven satellites at a perigee altitude of 8063 km, with a period of five orbits per day. This constellation, which is shown in Figure 5.1, is the setup for the simulations. The model used during the simulations is the one used in [16]. Note that this Thesis only uses the orbital mechanics and related modules, not the financial part of the model.

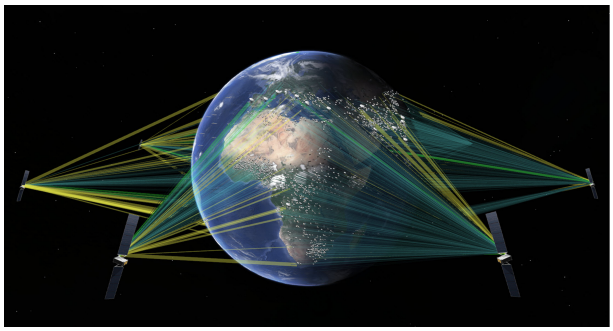

Figure 5.1: O3b mPower constellation.

5.2. Entities within the system

To model the problem, several classes have been defined within a system. They all follow a hierarchy, in the sense that, for instance, a Satellite $\mathcal{S}$ has a set of beams $\mathcal{B}$ linked to it,

and each of those beams has a set of carriers linked as well. Therefore, when one points out one element, there is the need of clarifying the super-elements where it belongs to uniquely define it.

Figure 5.2 shows this hierarchy and all the subclasses involved in a constellation.

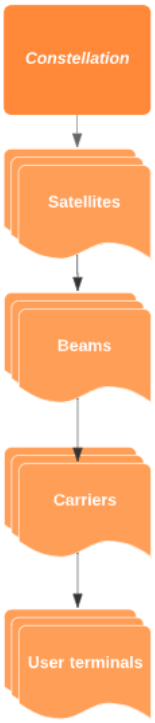

Figure 5.2: Hierarchy between the classes of the model.

5.2.1. User terminals

The user terminal is a class that stores information about each one of the receiving antennas. The main attributes of one user terminal are:

- Latitude: Latitude coordinate of the location of the antenna.
- Longitude: Longitude coordinate of the location of the antenna.
- Gain: Amount of gain, in dB, received by the beam.

For the following sections of this Thesis, elements of this class might be referred using a shorter version of the name: users or terminals.

5.2.2. Carriers

Carriers are a linking/container class. Each carrier contains a list of user terminals linked to it. It can be understood as a grouping of terminals.

5.2.3. Beams

Beams is a class that contains: on one side, a list of carriers linked to it, and on the other side, information about the transmitter antenna. The main attributes, therefore, are:

- Carriers: List of carriers assigned to a beam.
- Latitude: Latitude coordinate of the location of the projection of the center of the beam.
- Longitude: Longitude coordinate of the location of the projection of the center of the beam.
- Cone angle (θ_{3dB}): Beamwidth angle, as defined in Chapter 3.2.2. Sometimes is useful to refer to the half-cone angle ($\frac{\theta_{3dB}}{2}$).
- G_{max}: Maximum gain provided by the beam, in dB. Equivalently, the gain that a user completely centered would receive. It is the independent term (b) in Equation 5.3.5.
- D: Diameter of the reflector of the antenna, in meters. Its relation with θ_{3dB} can be seen in Equation 3.2.3
- Scanning loss: Loss of maximum gain with respect to a beam aligned with the nadir vector of the satellite. It is the loss due to the steering direction of the beam.
- Gain distribution: Equation mapping a direction θ with respect to the boresight to a gain value provided by the antenna. Equation 5.3.5 is used to model this distribution.

5.2.4. Satellites

Satellites is a class storing both physical attributes of the satellite and a list of beams. In particular, its main attributes are:

- Position: Coordinates of the satellite, available in different reference frames, mainly ECEF or ECI (Earth-centered inertial, respectively).
- Beams: List of beams linked to the satellite.

One main difference between this class and the other presented subclasses, is that its attributes depend on the time of the simulation. The users are static, the beams always point towards the same point (so, the beam itself changes but not its latitude and longitude); however, as the satellite moves, its position changes with time. Also, the beams linked to a satellite change with time.[1]

[1]This process of changing beams from satellite to satellite is called handover. There are different ways to carry out this, and the one used in the model of [16] is used. In summary, it decides to whose satellite goes each beam at a given time based on the proximity to the locations of gateways.

Parameter	Value
G_{max} [dB]	40
$\theta_{3dB}/2$ [º]	1.0
D [m]	0.52
f [GHz]	20
η [-]	0.83

Table 5.1: Transmitter antenna parameters for the simulation.

5.2.5. Constellation

Constellation is the highest-level class, containing the information of all its elements. Its main attributes are:

- Satellites: List of satellites within the constellation.
- Beams: List of beams within the constellation.

5.3. Modeling of the antenna

As the aim of the formulations presented in Chapter 4 is to optimize the provided gain, the transmitter antenna needs to be modeled.

5.3.1. Parameters

As the constellation that is used is in MEO orbit, a reasonable value for the minimum beamwidth of an antenna is $\theta_{3dB} = 2.0^{\text{o}}$. Then, the smallest half-cone angle used in this Thesis is $\theta_{3dB}/2 = 1.0^{\text{o}}$.

Considering a frequency of 20 GHz, (typical for Ka-band downlink [31]), with Equation 3.2.3, we get a diameter of the reflector of $D = 0.52$ [m].

To fully characterize the antenna, there is still another parameter to set: the maximum gain (or gain at boresight). Based on [32], a reasonable value is 40 dB. Thus, with Equation 3.2.1, the efficiency of the antenna is known and its value is $\eta = 0.83$.

These parameters are summarized in Table 5.1.

5.3.2. Scanning loss

One loss that needs to be modeled is the scanning loss, which is due to the beam not being pointing towards the nadir direction of its satellite. It can be understood as part of the L_{TX} loss of Chapter 3.4.2. It is a function of the scanning angle: the angle between the nadir direction of the satellite and the direction of the beam (when the scanning angle is 0º, the value of this loss is 0).

In terms of maximum value or behaviour of this loss, it highly depends on the antenna's design. As such design is not the focus of this Thesis, an approximation is considered. In particular, the value of the scanning loss will be taken to have the same order of magnitude as the pointing loss (from 0 to 3 dB). As a MEO constellation with the altitude considered in this Thesis won't have values of scanning angle higher than 25º, because it would be pointing outside the Earth, the modeling of the scanning loss follows Equation 5.3.1. The rationale behind this approximation is to have a value of zero in $scanningAngle = 0º$, and a value of 3 dB in $scanningAngle = 3º$.

$$L_{scan} = 30 \cdot (1 - cos(\text{scanningAngle})) \quad [dB] \tag{5.3.1}$$

5.3.3. Adding shape to the gain distribution

With the current model of the antenna, we already have different shapes for the beams. Note that the scanning loss affects the maximum gain (by reducing it), and, by Equation 3.2.1, it also affects the beamwidth (by increasing it). Then, as the model is right now, we have a minimum value of beamwidth of 2.0º, which corresponds to the beamwidth of a beam with no scanning loss (pointing towards the nadir direction of the satellite). If that beam points towards another direction, the gain distribution gets flattened (straightforward to see in Equation 3.2.4, as the maximum gain decreases and the beamwidth increases).

However, this means that the shape is uniquely defined by the pointing direction of the beam, and the aim of the Thesis is to take the shape as a degree of freedom. This is done by artificially reducing the diameter of the reflector by a factor named k.

In particular, one can get from Equation 3.2.1 the following:

$$D = \frac{c}{\pi f}\sqrt{\frac{10^{G_{max}/10}}{\eta}} \tag{5.3.2}$$

Where G_{max} is affected by the scanning loss.

Then, the idea is to add a factor to Equation 5.3.2 and get Equation 5.3.3:

$$D = \frac{c}{\pi f}\sqrt{\frac{10^{G_{max}/10}}{\eta}} \cdot k \tag{5.3.3}$$

The natural constraints for this parameter are: $k \in (0, 1]$; as a wider diameter than the physically constructed does not make any sense. In terms of beamwidth, we have a minimum value for each scanning angle, and the wider the beam gets the flatter the gain distribution becomes.

A by-product of adding this parameter is that, by Equation 3.2.1, another term is added to the maximum gain of the distribution: $20 \cdot log_{10}(k)$. This term is always non-positive and only 0 when $k = 1$, which corresponds to the fact that wider beams produce worse maximum gain.

Finally, the gain distribution within a beam (the equivalent to Equation 3.2.4) is shown in Equation 5.3.4.

$$G(\theta, k) = 40 - 30 \cdot (1 - cosd(\text{scanningAngle})) + 20 \cdot log_{10}(k) - 12(\frac{\theta}{\theta_{3dB}})^2 \tag{5.3.4}$$

To make it easier to work with, it is simplified to:

$$G = a\theta^2 + b \tag{5.3.5}$$

With both a and b as functions of the pointing direction and shape of the beam.

6. Methodology

This chapter aims to explain the methodology followed to test and analyze the formulations shown in Chapter 4.

6.1. Beam placement algorithm

As explained in Chapter 4.2, the beam placement problem aims to cover the users minimizing the number of beams used, as a proxy of the usage of resources. The approach that is used in this Thesis is described in [4]. As it is an important piece of this work, however, a summary of it is presented in the following lines.

The algorithm finds the solution for the beam placement problem (with a given fixed shape) using graph theory. In particular, solving an edge clique cover problem.

A graph is built with the user terminals as nodes, and an edge between two of them exists if the maximum angle between them, as seen from a satellite, is less than the predefined half-cone angle. In other words, two nodes are connected if they can be covered by the same beam.

In graph theory, a clique is a subset of nodes such that every two distinct nodes are connected (i.e., the induced subgraph is complete). In this context, a clique is a group of terminals that can, pairwise, be in the same beam. Based on that, an approximation is made: a clique is a group of terminals that can be in the same beam[1]

The problem solved, then, it is an edge clique cover problem, where one aims to get a set of cliques that cover all the users, without overlapping, with the minimum number of them.

In terms of the algorithm, as the problem is known to be NP-Complete, it is solved

[1]This is true for most cases, but is an approximation, so technically coverage is not guaranteed. This fact is explored in Chapter 7.3.2.

using heuristics. The rationale behind the method used is to sort all the cliques in the graph by size, and start getting the bigger cliques, discarding the cliques that include already-covered terminals.

The main weak points of this approach are:

- The global optimum is not guaranteed.
- Some users can be not covered.

An example of a graph from an arbitrary set of terminals, along with the solution, are shown in Figures 6.1 and 6.2.

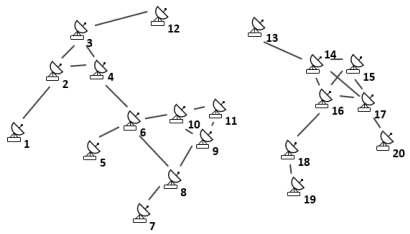

Figure 6.1: Graph built from a set of 20 terminals. Source: [4]

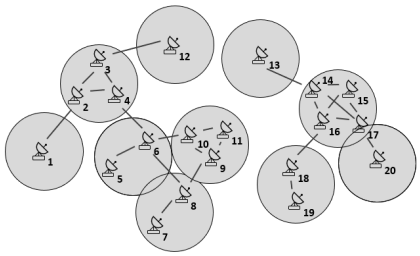

Figure 6.2: 10 beam placement for a set of 20 terminals. Source: [4]

In terms of performance of the system, an important note is that this approach does not consider the gain distribution of the beams at all. Thus, in that sense, the solution is sub-optimal in terms of gain.

6.2. Conservative beam placement algorithm

Based on the previous algorithm, we define an slightly different method that is used to compare our results. It consists in applying the same algorithm but, when building the graph -and only then-, use $\theta_{2dB}/2$[2] instead of $\theta_{3dB}/2$. This way, as the geometrical considerations are carried out using a smaller angle, the user terminals tend to be more centered,

[2]The half-cone angle using a 2dB cutoff definition.

farther from the edges of the beams. Thus, reducing the pointing loss at the expense of using a greater number of beams. This approach is over-conservative in the sense that tries to ensure that all the user terminals are really inside the beam, that is why it will be referred to as *Conservative beam placement*.

The rationale behind using this method is that is straightforward to apply having already the beam pointing algorithm, it does not require any other optimization process. So, if the results are equal or better than our approaches, this method could be preferable.

6.3. Gradient Descent technique

Gradient Descent is an iterative optimization algorithm for finding the minimum of a differentiable function. Given a first point a_0, the next elements are computed as follows:

$$a_{n+1} = a_n - \gamma \nabla F(a_n)$$

where $\gamma > 0$ is a parameter called the learning rate.

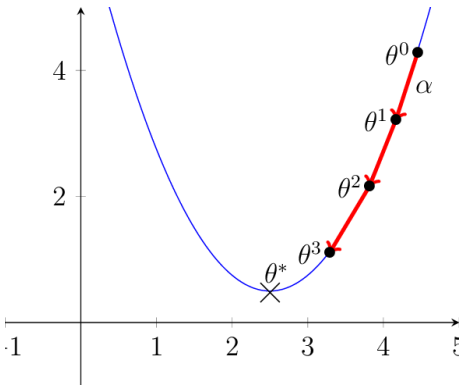

Figure 6.3: Gradient descent iterative procedure visualization. Source: [5].

This technique consists, as one can see from Equation 6.3 and Figure 6.3, in taking steps in the opposite direction to the gradient of the function. In this way, one moves towards lower values.

Note that, if the objective is to find the maximum of a function, the gradient descent algorithm can be applied to $G = -F$.

One reason to carry out the optimization process of the Thesis using Gradient Descent is because of its speed, which is important for an optimization of thousands of variables. Additionally, it synergizes well with the joint problem we are trying to solve.

This is due to the fact that the solution depends on the initial point, and the idea of our solution, as it has been explained in Chapter 4, is to modify the outcome of the beam placement problem. Having a good guess as a initial point, not just using a random feasible point, is called having a warm start, and it is a common practice when applying Gradient Descent.

While those are pros of the gradient descent, there are also cons that one has to take into account. The main shortcoming of the algorithm is that it can get stuck in local minima if the function F is not convex. Therefore, getting the global optimum of the function is not guaranteed, in general.

6.3.1. Applying gradient descent to the local formulation

As it was introduced in Chapter 4.5, for each beam b, we have a function $\mathcal{G}_b$ to optimize:

$$\mathcal{G}_b = \sum_{u \in \mathcal{U}_b} \bar{G}(b, u)$$

As the variables to optimize are (ϕ_b, θ_b, k_b):

$$\nabla \mathcal{G}_b = \left[\frac{\partial \mathcal{G}_b}{\partial \phi_b}, \quad \frac{\partial \mathcal{G}_b}{\partial \theta_b}, \quad \frac{\partial \mathcal{G}_b}{\partial k_b} \right]^T$$

The gradient, then, is:

$$\begin{array}{l} \frac{\partial \mathcal{G}_b}{\partial \phi_b} = \sum_{u \in \mathcal{U}_b} \frac{\partial \bar{G}(b,u)}{\partial \phi_b} \\ \frac{\partial \mathcal{G}_b}{\partial \theta_b} = \sum_{u \in \mathcal{U}_b} \frac{\partial \bar{G}(b,u)}{\partial \theta_b} \\ \frac{\partial \mathcal{G}_b}{\partial k_b} = \sum_{u \in \mathcal{U}_b} \frac{\partial \bar{G}(b,u)}{\partial k_b} \end{array} \tag{6.3.1}$$

Which is straightforward to compute using the analytical formulation shown in Equation 5.3.5. The exact formulae can be found in Appendix A.

6.3.2. Applying gradient descent to the global formulation

In Chapter 4.6, a formulation has been presented that is not differentiable, as $X_{b,u}$ is a discrete (non-continuous) variable:

$$\mathcal{G}(\mathcal{B}) = \sum_{b \in \mathcal{B}} \sum_{u \in \mathcal{U}} \bar{G}(b, u) X_{b,u} \tag{6.3.2}$$

In order to apply Gradient Descent, an alternative formulation has been used. In particular, the role that $X_{b,u}$ plays (avoid overlapping) is carried out outside of the Gradient Descent. That is, the gradient descent allows overlapping, but the algorithm will remove *unnecessary beams*[3]. More details on that in Chapter 6.4.2.

[3]A beam that is part of the outcome of the gradient descent step is considered unnecessary if does not have any user linked to it. For instance, if it's completely overlapping with another beam and that set of terminals is linked to it.

Thus, the objective function ends up being:

$$\mathcal{G}(\mathcal{B}) = \sum_{b \in \mathcal{B}} \sum_{u \in \mathcal{U}} \bar{G}(b, u) \tag{6.3.3}$$

The gradient, in this global formulation, is:

$$\nabla \mathcal{G} = \left[\frac{\partial \mathcal{G}}{\partial \phi_1}, \frac{\partial \mathcal{G}}{\partial \theta_1}, \frac{\partial \mathcal{G}}{\partial k_1}, \frac{\partial \mathcal{G}}{\partial \phi_2}, \frac{\partial \mathcal{G}}{\partial \theta_2}, \frac{\partial \mathcal{G}}{\partial k_2}, ..., \frac{\partial \mathcal{G}}{\partial \phi_b}, \frac{\partial \mathcal{G}}{\partial \theta_b}, \frac{\partial \mathcal{G}}{\partial k_b}, ..., \frac{\partial \mathcal{G}}{\partial \phi_{N_b}}, \frac{\partial \mathcal{G}}{\partial \theta_{N_b}}, \frac{\partial \mathcal{G}}{\partial k_{N_b}} \right]^T$$

The gradient, then, is:

$$\begin{array}{l} \frac{\partial \mathcal{G}_b}{\partial \phi_b} = \sum_{b \in \mathcal{B}} \sum_{u \in \mathcal{U}} \frac{\partial \bar{G}(b,u)}{\partial \phi_b} \\ \frac{\partial \mathcal{G}_b}{\partial \theta_b} = \sum_{b \in \mathcal{B}} \sum_{u \in \mathcal{U}} \frac{\partial \bar{G}(b,u)}{\partial \theta_b} \\ \frac{\partial \mathcal{G}_b}{\partial k_b} = \sum_{b \in \mathcal{B}} \sum_{u \in \mathcal{U}} \frac{\partial \bar{G}(b,u)}{\partial k_b} \end{array} \tag{6.3.4}$$

6.4. Algorithms overview

With the gradients defined and computed for both formulations, this next chapter presents the algorithms to carry out the joint optimization. As each formulation is a different framework of the problem, they deal with different issues, and thus the algorithms are significantly different.

6.4.1. Algorithm for the local formulation

The local formulation has the most straightforward algorithm. As it is a fine-tuning of the outcome of the beam placement problem, the mapping between users and beams is defined, and one does not have to deal with overlapping or not covered users, as it happens in the global formulation.

As it has been previously introduced, the first point is a warm start from the heuristic beam placement. The process is as in Figure 6.4.

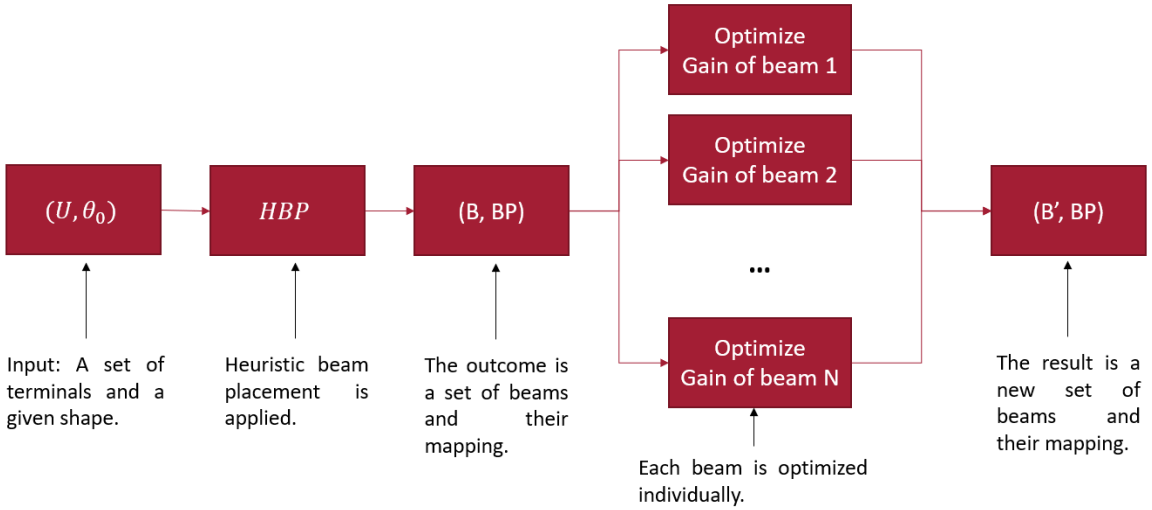

Figure 6.4: Local optimization algorithm flowchart.

6.4.2. Algorithm for the global formulation

In the global formulation, the mapping between users and beams changes, and as in the gradient descent process the set of beams never changes its cardinality, it can happen that some users are left uncovered. Therefore, this needs to be checked.

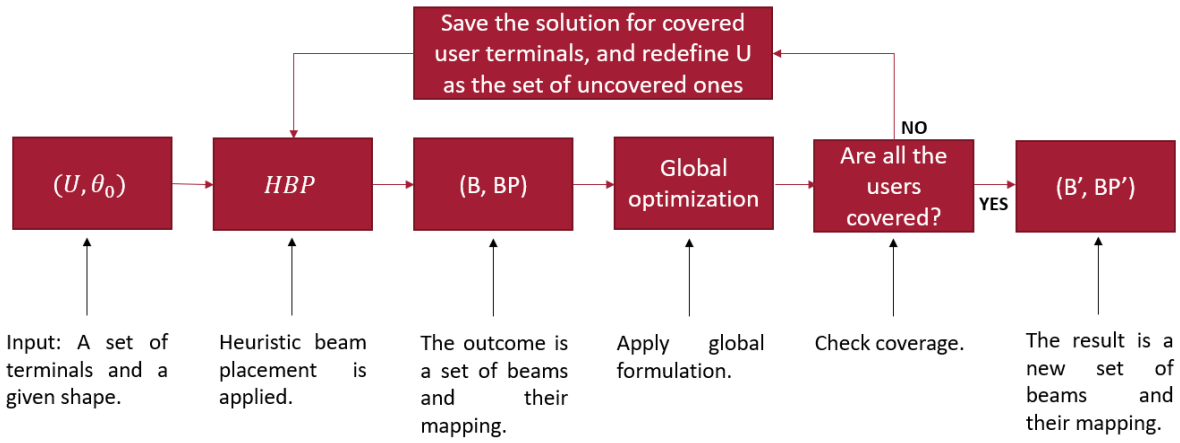

Figure 6.5: Global optimization algorithm flowchart.

The proposed algorithm to tackle the global formulation is shown in Figure 6.5. It is essentially to carry out the same optimization process with the addition of checking the coverage at the end and building a loop. This loop consists in getting the solution of the Gradient Descent and extracting the set of beams and covered users, running again the

placement for the uncovered users.

In the first iteration of the loop, the heuristic beam placement is carried out with the whole set $\mathcal{U}$ and the Gradient Descent process is applied to its outcome. Let's suppose that, this outcome, consists in a set of beams $\mathcal{B}_0$ and a subset $\mathcal{U}_0 \subset \mathcal{U}$ of users covered. The idea of the loop is to apply the same process to $\mathcal{U}' = \mathcal{U} \setminus \mathcal{U}_0$, getting another set of beams $\mathcal{B}_1$. This process will be ran until every user is covered, so it can be ran several times (it is straightforward that it finishes).

In general, we get several sets of beams: $\mathcal{B}_0$, $\mathcal{B}_1$, $\mathcal{B}_2$, etc. The final set of beams is, then, $\mathcal{B} = \cup_{\forall i}\mathcal{B}_i$. And the final mapping between users and beams is the natural "union" of the placements for each loop:

$$BP(u) = \begin{cases} BP_0(u) & u \in \mathcal{U}_0 \\ BP_1(u) & u \in \mathcal{U}_1 \\ BP_2(u) & u \in \mathcal{U}_2 \\ ... & ... \end{cases}$$

Which is well-defined as the set of $\mathcal{U}_i$ is a partition of $\mathcal{U}$.

6.5. Simulations methodology

As the heuristic beam pointing algorithm needs a half-cone angle as an input, and all the other approaches need to run that algorithm to work, the simulations are carried out doing a swipe through different inputs. That is, different half-cone angles. In particular, the smallest half-cone angle is the smallest acceptable by the antenna (1.0^o) and it is increased by 0.05^o until 1.8^o.

For the smaller scenarios, the baseline -due to its heuristic nature- can be inconsistent. For instance, it can get a solution with more beams after increasing the half-cone angle. In bigger scenarios this sub-optimality doesn't affect that much the solution, as the difference is smaller. With this in mind, each algorithm is applied a number of times based on the size of the scenario. The results shown in Chapter 7 are, then, the average among all the runs of such algorithms.

For instance, for the local optimization method to be tested on Scenario 2 (see Test Cases in 6.7, this algorithm is ran four times, and all the metrics are the average through these four runs.

The number of trials for each scenario are summarized in Table 6.1.

Scenario	Number of user terminals	Number of trials
1	100	5
2	500	4
3	1000	3
4	5000	2

Table 6.1: Number of trials per simulation.

6.6. Metrics

The following metrics are used to assess how good is one result compared to others:

- Number of beams: minimization of usage of resources is always one of the objectives. The better the lower this value is.

$$\text{Nb} = |\mathcal{B}|$$

- Mean pointing loss [dB]: averaging of all the pointing losses within the user terminals. The better the lower this value is.

$$\text{Mean pointing loss [dB]} = \frac{1}{N_u} \sum_{\text{u user}} \text{PLoss}_u$$

- Mean Gain [dB]: averaging of all the gains provided to the user terminals. As the Mean pointing loss, the average is taken within the linear space. The better the higher this value is.

$$\text{Mean gain [dB]} = 10\log_{10}\left(\frac{1}{N_u} \sum_{\text{u user}} 10^{\frac{\text{Gain}_u}{10}}\right)$$

So, two particular solutions of the problem will be compared using these metrics. A solution will be clearly better than the other one if dominates it. To dominate, in this context, means to be better in all the metrics. If two solutions are compared and each one is better in one particular metric, no direct conclusion can be extracted from there.

6.7. Test cases

For the testing part, a realistic dataset provided by SES S.A. is used. This model allows us to get sets of terminals of a fixed size with a realistic distribution. In this Thesis, four scenarios are used, which are shown in Figures 6.6 - 6.9. The black dots represent the

user terminals and the triangles represent the projection of the satellites in a particular time snapshot.

Note that different scenarios not only represent differences in terms of size, but also in terms of densities. The effects of these parameters on the solutions are explored in Chapter 7 and Chapter 8.

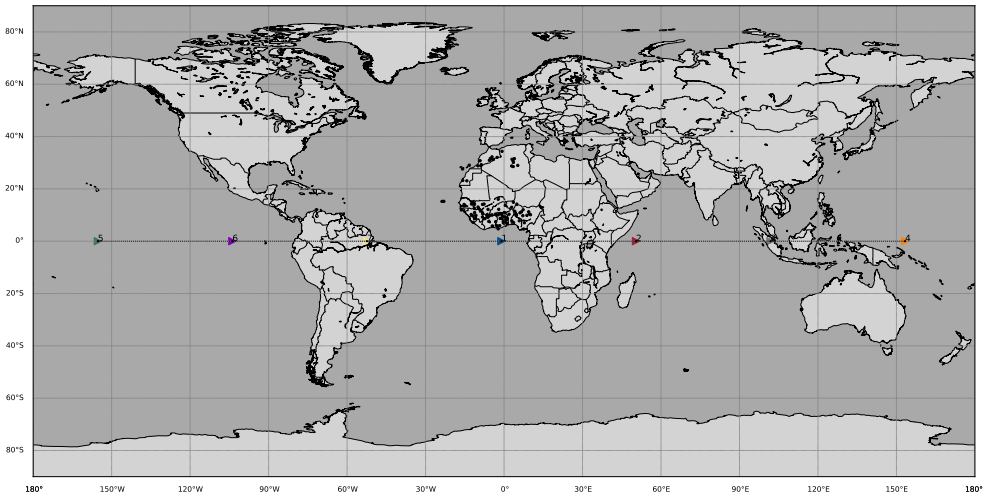

Figure 6.6: Scenario 1: 100 user terminals.

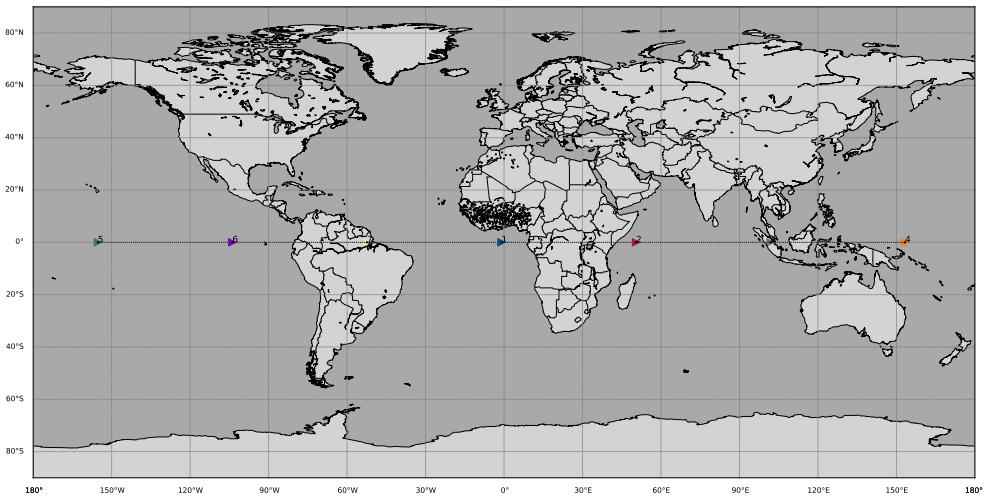

Figure 6.7: Scenario 2: 500 user terminals.

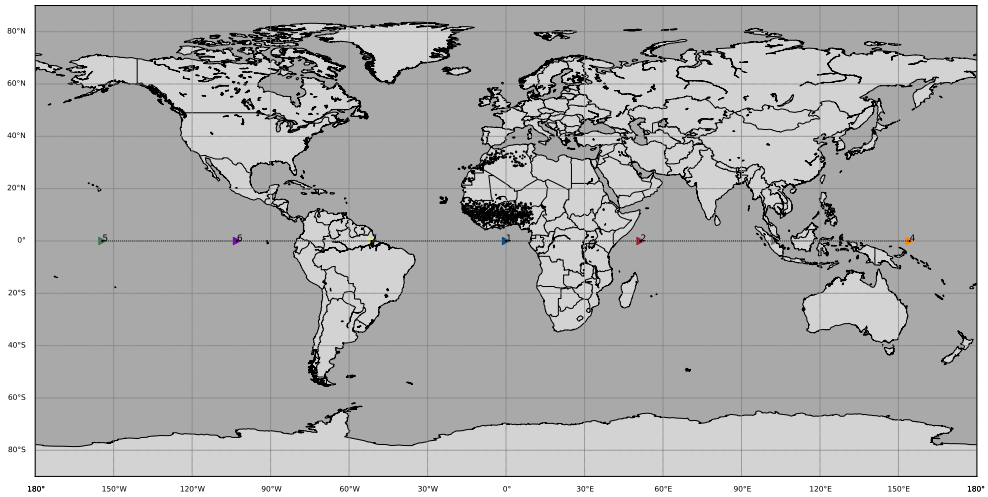

Figure 6.8: Scenario 3: 1000 user terminals.

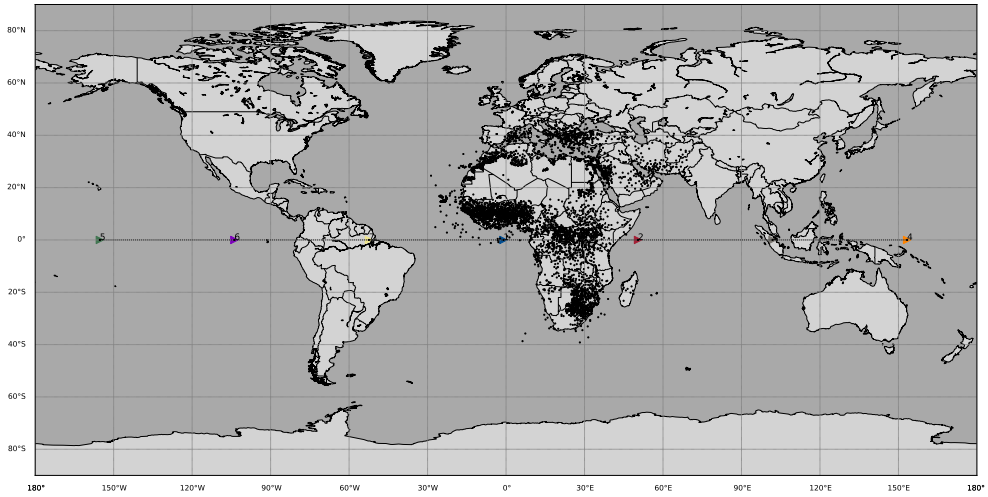

Figure 6.9: Scenario 4: 5000 user terminals.

6.8. Baseline

To compare the obtained results, one needs to first set a baseline. Then, one is able to benchmark how good is the studied approach.

The main baseline in this study is the result obtained with the beam pointing algorithm. As our approaches use the outcome of this algorithm, it is natural to compare them with it to measure the improvement that one has. The algorithm and the problem that it solves have been already explained in Sections 6.1 and 4.2, respectively.

7. Results

The aim of this Chapter is to present the obtained results with the different algorithms: conservative beam pointing (Chapter 6.2), local formulation (Chapter 6.4.1), and global formulation (Chapter 6.4.2). Each one will be bench-marked against the main baseline, the heuristic beam placement (Chapter 6.1), and comparisons between them are presented.

7.1. Mean gain [dB]

Figure 7.1 shows the mean gain [dB] as a function of the average half-cone angle of all the methods. We can see that, in this metric, Conservative placement > Global optimization > Local optimization > Heuristic placement.

- **Conservative beam placement** dominates the heuristic (baseline) approach. The rationale behind this is that, for the conservative method and given a half-cone angle, the user terminals tend to be more centered (as they have to fit in a smaller geometric contour) compared to the heuristic gain.Also, the improvement of the conservative approach does not depend on the density of the test case.

- **Local optimization** presents an small, but consistent, improvement with respect to the baseline in this metric.

- **Global optimization** reaches higher average gain than the baseline. Note that, for denser scenarios, the improvement in this metric gets lower. An explanation for this fact is provided in Chapter 7.5, when all the metrics have been presented.

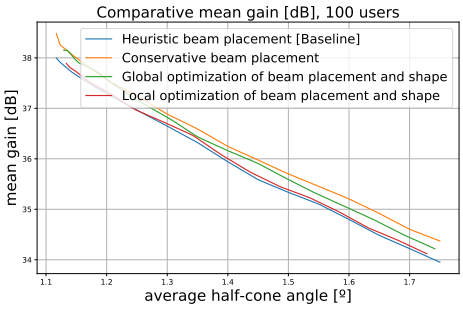

(a) Scenario 1: 100 user terminals.

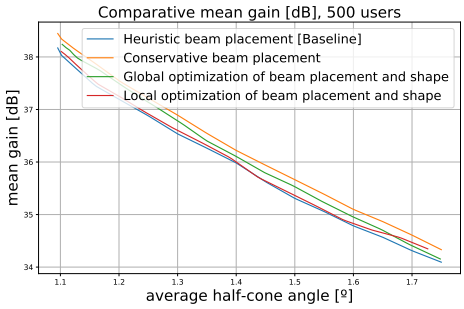

(b) Scenario 2: 500 user terminals.

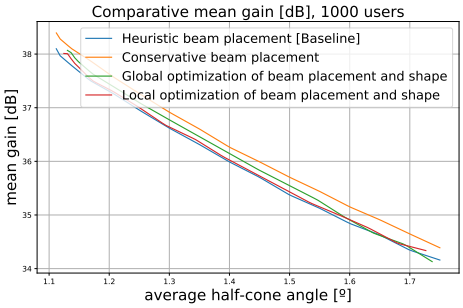

(c) Scenario 3: 1000 user terminals.

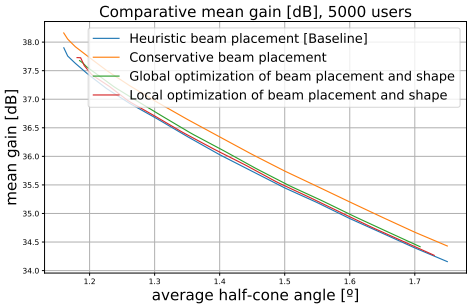

(d) Scenario 4: 5000 user terminals.

Figure 7.1: Mean gain [dB] as a function of the average half-cone angle [º] for all the methods against the baseline on all four scenarios.

7.2. Mean pointing loss [dB]

in Figure 7.2, the mean pointing loss [dB] as a function of the average half-cone angle of all the methods are shown. In this metric we see the same behavior[1], Conservative beam placement < Global optimization < Local optimization < Heuristic placement.

- **Conservative beam placement**'s behavior is the same than with mean gain. This is expected, as the shape is constant in these simulations (neither the heuristic nor the conservative beam placements change shape), and the pointing loss is the difference between the gain received and the maximum gain within a beam. Then, because the beam shape is constant, improving one metric improves the other one and by the same amount.

- **Local optimization** dominates the baseline achieving consistently smaller pointing losses [dB].

[1]Here, lower is better.

- **Global optimization** also dominates the baseline. It also happens that the improvement in average pointing loss gets smaller for denser scenarios, going from 0.25 dB (Figure 7.2a) to 0.1 dB (7.2d).

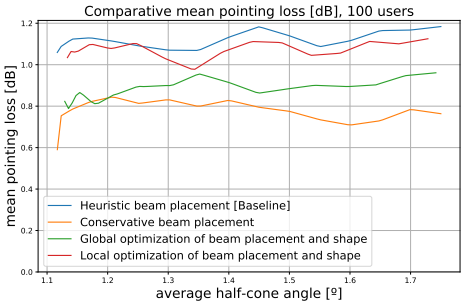

(a) Scenario 1: 100 user terminals.

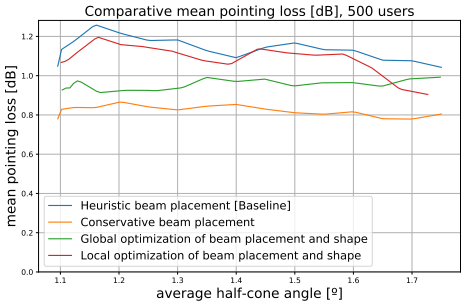

(b) Scenario 2: 500 user terminals.

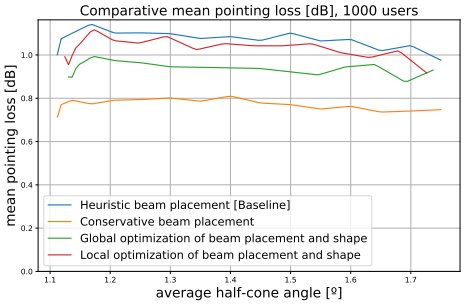

(c) Scenario 3: 1000 user terminals.

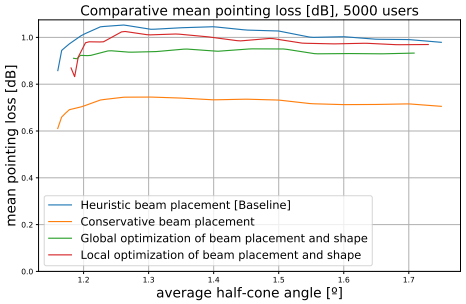

(d) Scenario 4: 5000 user terminals.

Figure 7.2: Mean pointing loss [dB] as a function of the average half-cone angle [º] for all the methods against the baseline on all 4 scenarios.

7.3. Coloring based on pointing loss

Apart from the metric value of the pointing loss, it helps to visualize what it means. Two color schemes for the beams has been defined in order to see the difference of results between all the methods with respect to the pointing loss.

The first scheme consists in the following: for each beam, one takes the pointing loss of every user terminal, and takes the mean over time (equivalently, over the full orbit). If this value is between 0 and 2 dB, the color assigned is green, representing that it is a *good enough* beam in this metric. If this value is between 2 and 3 dB, the color is orange, meaning that on average the user terminals are close to the edge of the beam. Otherwise, for values greater than 3 dB, it means that on average the user terminals are outside the beam, being colored in red. The distribution of colors gives us information about the average performance of the beams.

The second color scheme follows the same rule but using the maximum pointing loss

within the terminals in a beam (can be understood as worst case per beam) as the value to assign the color. So, in this case, orange means that there is at least one user terminal close to the edge. And, more importantly, red means that there is at least one user terminal outside of the beam at some time.

To show this analysis, as all the methods depend on the beam pointing algorithm, we fix a particular shape (i.e., a fixed θ_{3dB}) and a particular scenario (Scenario 4) before running the algorithms.

7.3.1. First coloring scheme

The results from applying the first coloring scheme to the outcome of all the algorithms are shown in Figures 7.3 - 7.6, along with the distributions of each color. With this scheme, all the methods seem to work really good, as all surpass 95% of green beams. In particular, conservative beam placement has all green, local optimization has only 2 orange beams, heuristic placement has 5 orange ones, and global 9 orange beams (4% of total beams).

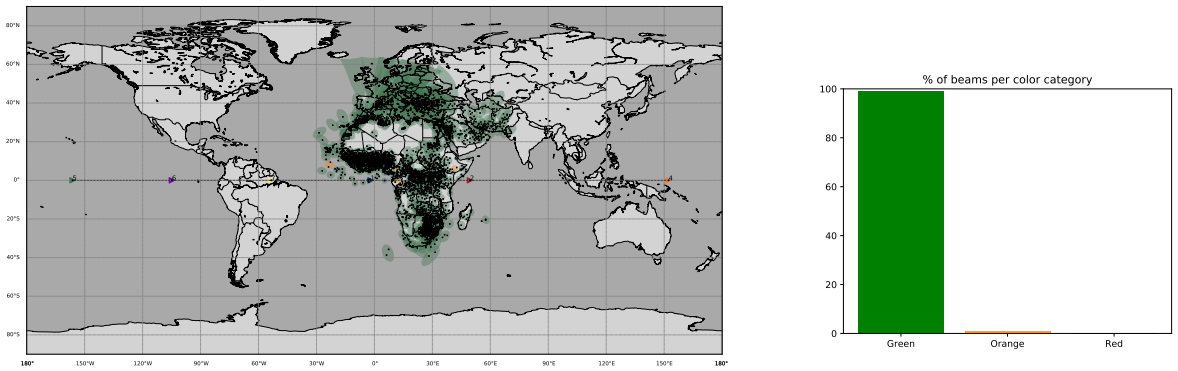

(a) Coloring scheme. (b) Distribution of colors.

Figure 7.3: First coloring scheme applied to the result of the heuristic beam pointing algorithm to Scenario 4.

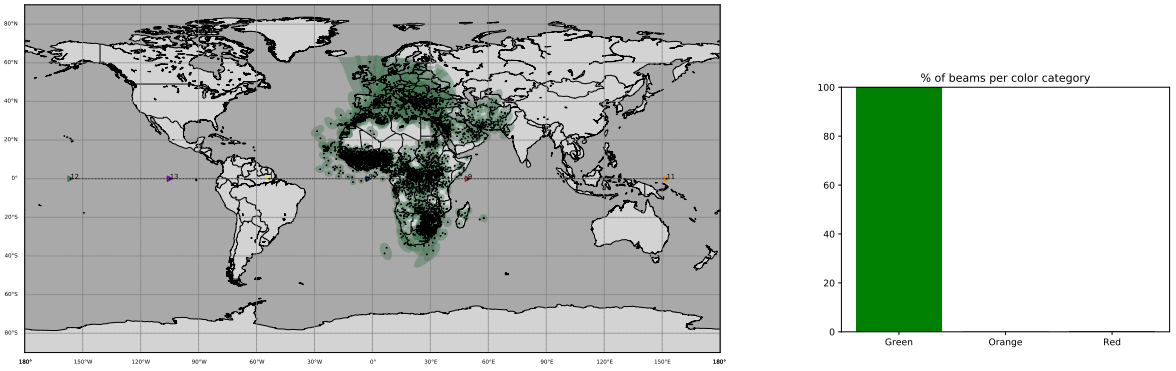

(a) Coloring scheme. (b) Distribution of colors.

Figure 7.4: First coloring scheme applied to the result of the conservative beam pointing algorithm to Scenario 4.

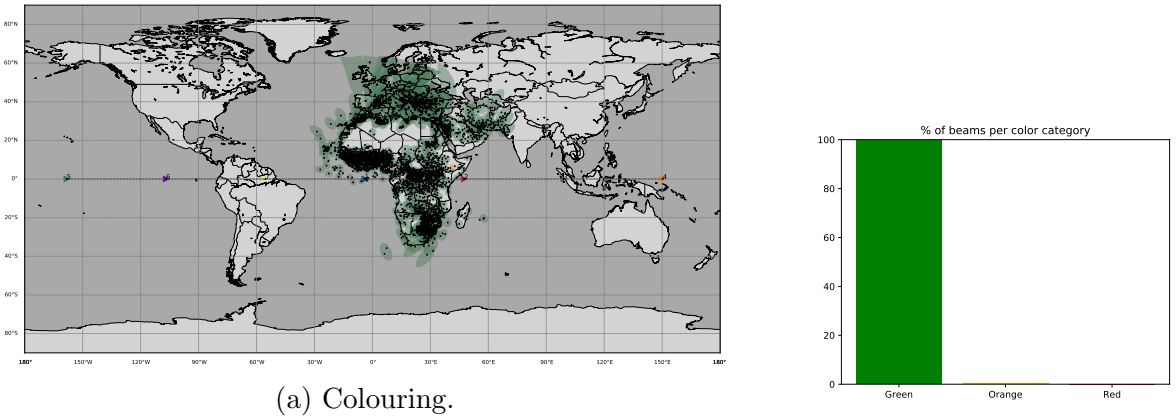

(a) Colouring.

Figure 7.5: First coloring scheme applied to the result of the local optimization algorithm to Scenario 4.

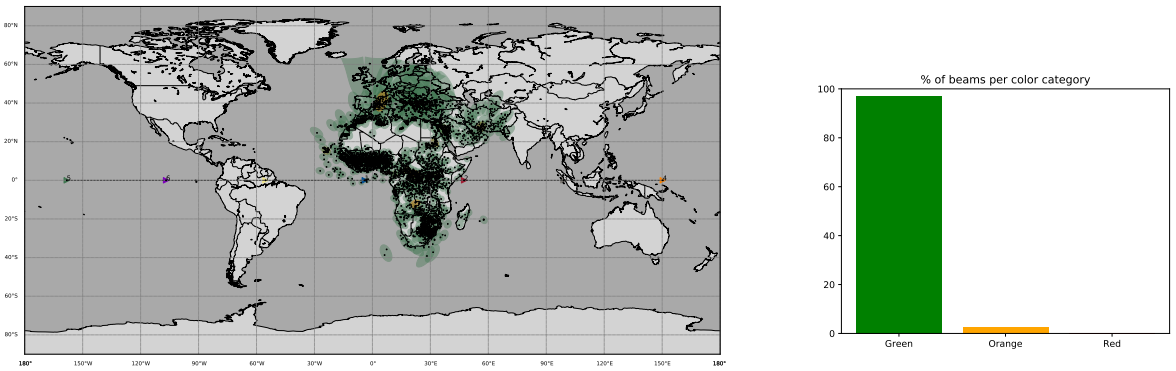

(a) Coloring scheme. (b) Distribution of colors.

Figure 7.6: First coloring scheme applied to the result of the global joint beam pointing and shaping algorithm to Scenario 4.

7.3.2. Second coloring scheme

The results from applying the second coloring scheme to the outcome of all the algorithms are shown in Figures 7.7 - 7.10, along with the distributions of each color. This second color scheme reveals more interesting information, as gives important insights for a operator to decide which method to use (red beams imply terminals not being covered). In this case, we can see that the heuristic placement has 20% of red beams, the local method 18 % the conservative beam placement 5 (2%), and global none. We also see that, when one studies worst-case performance per beam, the heuristic placement maintain 60% of green beams, the conservative approach 80%, the local 50%, and the global 40%.

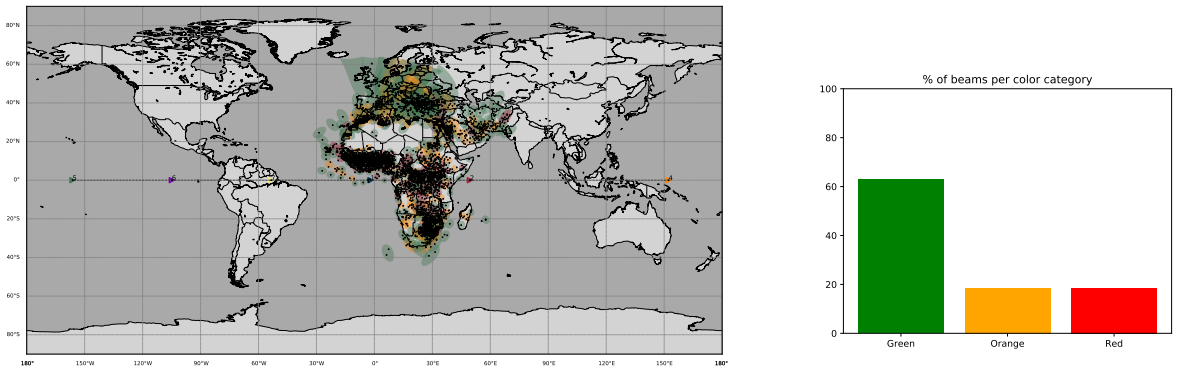

(a) Coloring scheme. (b) Distribution of colors.

Figure 7.7: Second coloring scheme applied to the result of the heuristic beam pointing algorithm to Scenario 4.

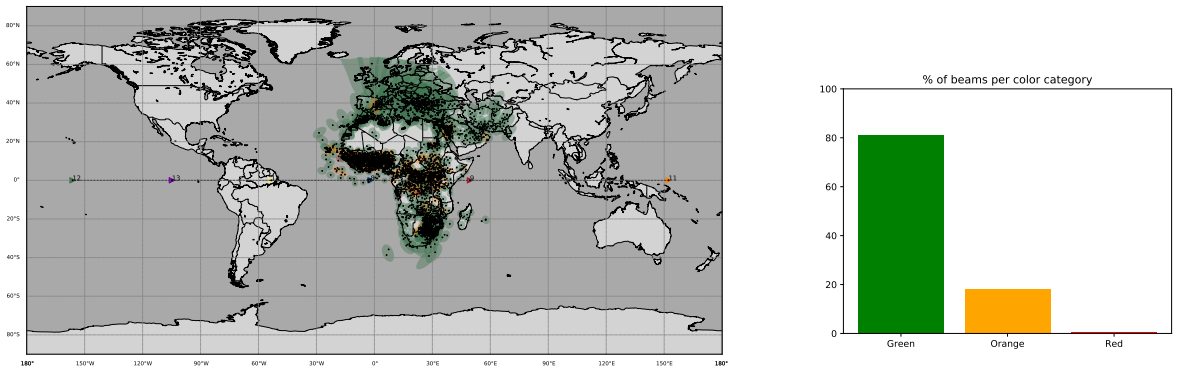

(a) Coloring scheme. (b) Distribution of colors.

Figure 7.8: Second coloring scheme applied to the result of the conservative beam pointing algorithm to Scenario 4.

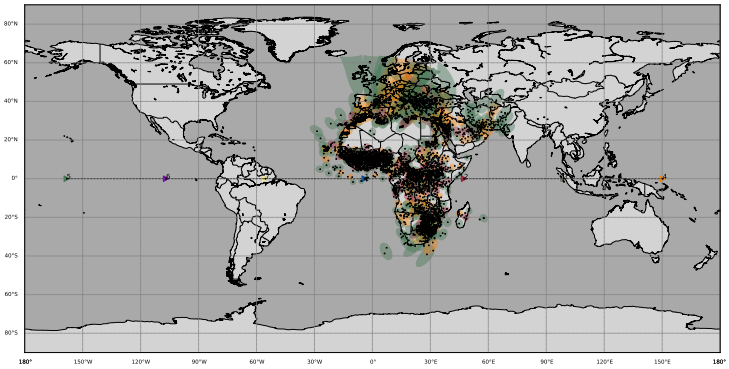

(a) Colouring.

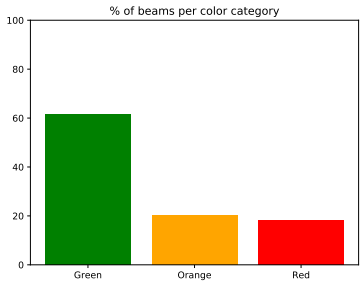

(b) Distribution of colours.

Figure 7.9: Second coloring scheme applied to the result of the local optimization algorithm to Scenario 4.

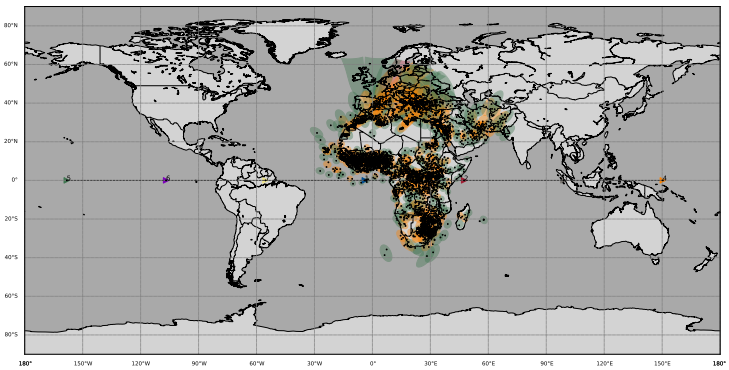

(a) Coloring scheme.

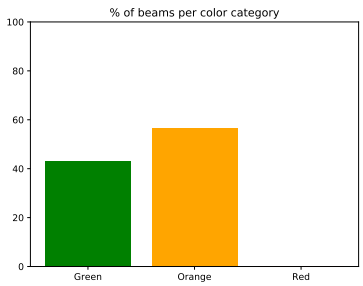

(b) Distribution of colors.

Figure 7.10: Second coloring scheme applied to the result of the global joint beam pointing and shaping algorithm to Scenario 4.

7.4. Number of beams

Figure 7.11 shows the comparison of all the methods with respect to the number of beams. Here, different behaviors are observed on different scenarios.

- **Conservative beam placement** is dominated by the heuristic approach. In this case, the relationship is straightforward to see. As the conservative approach computes the beams considering a contour with a half-cone angle $\sqrt{2/3}$ times smaller, the number of beams of the conservative approach for angle X should be the same[2] as the number of beams of the heuristic approach for angle $\sqrt{2/3}$X. For instance,

[2] As the heuristic placement uses a greedy approach, this fact is not true always. There is a small error as it does not find the global optimum.

in Scenario 1 (Figure 7.11a) we can see that the Conservative approach, for a half-cone angle of 1.6º, uses 26-27 beams; which is the same amount than the heuristic approach with 1.3º. It tends to use around 20% of extra beams.

- **Local optimization**'s number of beams is the same as in the baseline by definition. The only insight that we can extract from here is that the beams tends to be smaller, as the graphs of the local method are, basically, the baseline's shifted a bit to the left.

- **Global optimization**'s behaviour change along the scenarios. There are scenarios (i.e., Figure 7.11a) where the heuristic beam pointing clearly dominates, but in others (i.e., Figure 7.11d) is not the case. One can conclude that, for less dense scenarios, heuristic beam pointing does a better job in terms of using less beams. In denser scenarios, however, the global optimization can reach solutions with the same number of beams or even less.

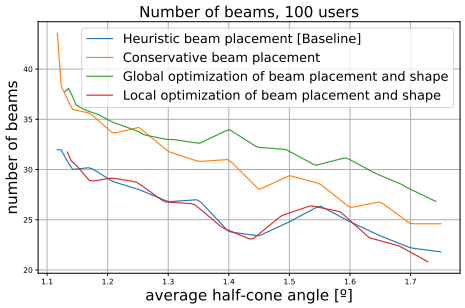

(a) Scenario 1: 100 user terminals.

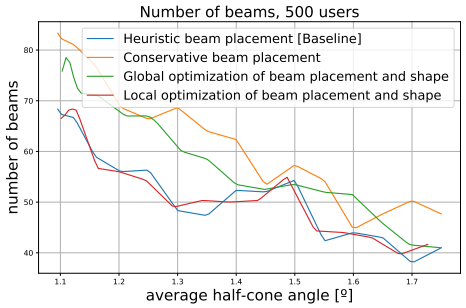

(b) Scenario 2: 500 user terminals.

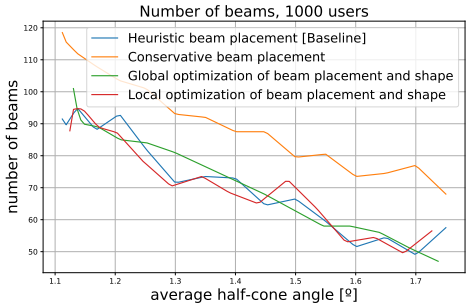

(c) Scenario 3: 1000 user terminals.

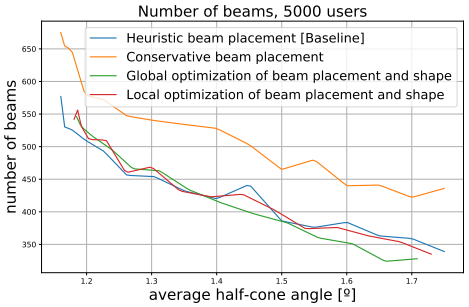

(d) Scenario 4: 5000 user terminals.

Figure 7.11: Number of beams as a function of the average half-cone angle [º] for all the methods against the baseline on all 4 scenarios.

7.5. Summary

The analysis of the three methods can be summarized as follows:

- **Conservative beam pointing** is a good method to guarantee a better performance, but always at the expense of adding more beams. It is able to improve the

pointing loss by 0.3 dB on average, approximately, but adding 20% more beams. Another shortcoming from this method is that it does not guarantee coverage for all the user terminals, as it has been seen in 7.3.2.

- **Local optimization**, as it is a fine-tuning of the beams, improves with respect to the first two metrics without the downside of adding more beams. The improvement, as it has been compared, is smaller than the other methods. Additionally, it has the same coverage problem as the heuristic placement.

- **Global optimization** method is able to consistently perform better in terms of gain and pointing loss, regardless of the scenario. In terms of number of beams, it shines in denser scenarios, while in sparse scenarios tends to use more beams.

  This last fact and the lowering of improvement in the first two metrics are easily understood if one thinks in the coverage constraint of the global method. If we take Scenario 4 as an example, we see in Chapter 7.3.2 that the baseline has 20% of the beams with, at least, one user not covered. Then, the global method finds a solution that, with the same or even less beams, covers all the users. One can expect the lower improvement as, with the same resources, it has to take care of more uncovered terminals.

8. Conclusion

This final chapter aims to summarize the key findings of this Thesis and address the research questions posed at the start. Opportunities of future research are also introduced.

8.1. Thesis summary

Chapter 1 began by presenting the context and motivation of the Thesis, along with the research objectives being pursued. Then, in Chapter 2 the literature review was conducted on the main topics of interest of the thesis, providing at the end a summary of the literature with respect to these topics.

Chapter 3 provides the necessary background in satellite communications to follow the thesis, from the definition of what is a link to how to compute it and the role that the gain of the transmitter antenna plays. It also goes through the advantages and disadvantages of multi-beam satellite systems. In Chapter 4, the joint optimization of beam placement and shape problem is formulated. First, giving a definition of both problems individually, and, later, tackling the joint problem with two different formulations.

Chapter 5 describes the model being used: the MEO constellation of satellites, the architecture of entities within the model, the design of the antenna being used, and its gain distribution. It is in Chapter 6 where the methodology of the simulations is explained, from the baseline to the algorithms, the metrics, test cases, etc.

The results of this methodology are shown in Chapter 7, where one can see the performance of each method with respect to each of the metrics and a comparison between them, analyzing all the nuances and the dependence of the results on the test cases.

8.2. Executive summary of results

This chapter summarizes the results obtained in answering the two research questions introduced in Chapter 1.2.

8.2.1. Research question 1

Research question 1

What is the value of the joint optimization of beam placement and shaping for multi-beam satellite constellations?

The analysis of the results of Chapter 7 shows that algorithms that optimize only pointing (heuristic and conservative) either get a sub-optimal gain distribution with a low number of beams or they get an improvement at the expense of adding more beams. The local formulation shows that there can be some fine-tuning optimizing both pointing and shape, allowing a little improvement using the same number of beams. However, it is with the global formulation that we have proved that one can get an improvement in terms of gain with the same number of beams, even with less in some cases. And this fact only gets enhanced by the fact that this last formulation had a constraint that the other three hadn't, which is always covering the whole set of user terminals (as seen in Section 7.3.2).

In that sense, the answer is clear: we can get improvement on gain and pointing loss while maintaining (or even reducing) the usage of power resources (in this Thesis, the number of beams has been used as a proxy for it).

However, we have seen that this fact depend on the test scenario: It is in the denser scenarios when this answer holds true. In sparser ones (such as scenarios 1 and 2), the joint optimization provides improvement of performance at the expense of higher usage of resources.

Then, as seen from a hypothetical company perspective, the conclusion would be: if you are a major satellite operator with thousands of user terminals in a dense distribution, then the joint optimization can make a difference and get an improvement from it; however, if you are an operator that, for instance, some of your clients are container ships over the Pacific, which tends to be a sparse set, then there is no much room for improvement there apart from assigning a beam to each ship and making the smallest shape (to get maximum gain).

8.2.2. Research question 2

Research question 2

In the context of gain optimization for multi-beam satellite constellations, is Gradient Descent a suitable optimization method?

Based on the results of Chapter 7, the algorithms that used Gradient Descent have been proved to reach their aim. So, in that sense, as the Thesis has developed an analytical, continuous, and differentiable expression for the gain, the Gradient Descent technique has

been found helpful and useful to optimize that parameter.

It has also allowed to bring two different approaches, which can correspond to different situations in business: the global formulation if one is able to define the locations of all beams to start a service, and the local formulation if the company is in the middle of a service and is not able to make big changes in the beams' configuration (for instance, the link routing from terminals to beams).

At the same time, when carrying out this optimization one can consider more parameters, such as the demand of the terminals (as it is explained in Future Work, Chapter 8.3). Some of these parameters can be easily added to the formulation and be solved with the same technique. So, gradient descent has the potential to be expanded to more complex formulations of the problem.

Thus, the answer to this second research question is affirmative: Gradient Descent has been proved to be a suitable optimization technique to carry out gain optimization for a multi-beam satellite constellation.

8.3. Future work

In this chapter, possible extensions of this work and topics not explored in this Thesis are presented:

- **Introduce demand.**

  In this Thesis, the gain of the user terminals has been optimized without considering their demand in data rate. However, the demand plays an important role in the link budget equation, so it would be interesting to try to add this concept into the formulation.

  One way could be to just put weights in the sums of Equations 4.5 and 4.6.1 based on the demand value. Having said that, it is not clear if one should take the instantaneous demand, or its time average, or its peak, etc.

- **Study of the effect of density to beam pointing and beam shaping.**

  The improvement from these optimization methods shown in the thesis depend heavily on the density of user terminals, as it has been already shown. Thus, an interesting study would be to analyze in more details the improvement of these methods as a function of density and try to reach conclusions on when it is worth to apply them and when it is not.

- **Tackle the dynamic problem.**

  In the presented method, a beam is defined by its location and shape. And these parameters are fixed in time. However, current technologies allow to change them dynamically, allowing the system to adapt even better to the situation. Then, another natural extension of this work, more ambitious, is to tackle this dynamic problem where the outcomes are the variables that define the beam as functions of time.

  One should be aware of the constraints given by technology. For instance, maybe the beam pointing direction can change continuously but not the shape. Additionally, one has to take care of tracking correctly the beams with respect to the satellite they come from. As instantaneous handovers do not exist, maybe one has to force beams to overlap to take cover of the users while one beam is in the middle of handover.

Appendices

A. Gradient computation

The aim of this appendix chapter is to compute the analytical formulation of the gradient. The equation whose gradient we are interested in is the following:

$$G(\phi_b, \theta_b, k_b) = a\alpha^2 + b$$

Where the location of the user is fixed, and also the satellite to which the beam is linked.

With this in mind, we aim to compute the following derivatives:

$$\begin{aligned}
\frac{\partial G}{\partial \phi_b} &= \frac{\partial a}{\partial \phi_b}\alpha^2 + 2a\alpha\frac{\partial \alpha}{\partial \phi_b} + \frac{\partial b}{\partial \phi_b} \\
\frac{\partial G}{\partial \theta_b} &= \frac{\partial a}{\partial \theta_b}\alpha^2 + 2a\alpha\frac{\partial \alpha}{\partial \theta_b} + \frac{\partial b}{\partial \theta_b} \\
\frac{\partial G}{\partial k_b} &= \frac{\partial a}{\partial k_b}\alpha^2 + 2a\alpha\frac{\partial \alpha}{\partial k_b} + \frac{\partial b}{\partial k_b}
\end{aligned}$$

A.1. Alpha and its derivatives

The aim of this section is to find the derivatives of α, being it the angle between the position vectors of a terminal and a beam as seen from a satellite. In particular, lets assume we have the following three entities:

- A user u with coordinates (latitude, longitude) = (ϕ_u, θ_u).
- A beam b with coordinates (latitude, longitude) = (ϕ_b, θ_b).
- A satellite s with ECEF coordinates (x, y, z) = (x_s, y_s, z_s).

Let's define the three main points:

$$\begin{aligned}
U &= R(cos(\phi_u)cos(\theta_u), cos(\phi_u)sin(\theta_u), sin(\phi_u)) \\
B &= R(cos(\phi_b)cos(\theta_b), cos(\phi_b)sin(\theta_b), sin(\phi_b)) \\
S &= (x_s, y_s, z_s)
\end{aligned}$$

The vectors $\vec{SU}$ and $\vec{SB}$ (terminal and beam as seen from the satellite) are:

$$\vec{SU} = (\underbrace{Rcos(\phi_u)cos(\theta_u) - x_s}_{x_1}, \underbrace{Rcos(\phi_u)sin(\theta_u) - y_s}_{y_1}, \underbrace{Rsin(\phi_u) - z_s}_{z_1})$$

$$\vec{SB} = (\underbrace{Rcos(\phi_b)cos(\theta_b) - x_s}_{x_2}, \underbrace{Rcos(\phi_b)sin(\theta_b) - y_s}_{y_2}, \underbrace{Rsin(\phi_b) - z_s}_{z_2})$$

And we rename the coordinates as:

$$\vec{SU} = (x_1(\phi_b, \theta_b), y_1(\phi_b, \theta_b), z_1(\phi_b, \theta_b))$$
$$\vec{SB} = (x_2(\phi_b, \theta_b), y_2(\phi_b, \theta_b), z_2(\phi_b, \theta_b))$$

Note that, in fact, x_1, y_1 and z_1 are constant with respect to our variables (ϕ_b, θ_b).

The partial derivates that will be needed are:

$$\begin{array}{cc} \frac{\partial x_1}{\partial \phi_b} = 0 & \frac{\partial x_1}{\partial \theta_b} = 0 \\ \frac{\partial y_1}{\partial \phi_b} = 0 & \frac{\partial y_1}{\partial \theta_b} = 0 \\ \frac{\partial z_1}{\partial \phi_b} = 0 & \frac{\partial z_1}{\partial \theta_b} = 0 \\ \frac{\partial x_2}{\partial \phi_b} = -Rsin(\phi_b)cos(\theta_b) & \frac{\partial x_2}{\partial \theta_b} = -Rcos(\phi_b)sin(\theta_b) \\ \frac{\partial y_2}{\partial \phi_b} = -Rsin(\phi_b)sin(\theta_b) & \frac{\partial y_2}{\partial \theta_b} = Rcos(\phi_b)cos(\theta_b) \\ \frac{\partial z_2}{\partial \phi_b} = Rcos(\phi_b) & \frac{\partial z_2}{\partial \theta_b} = 0 \end{array}$$

Using the dot product of these two vectors, we know that the angle α between $\vec{SU}$ and $\vec{SB}$ is:

$$\alpha = cos^{-1}\left(\frac{< \vec{SU}, \vec{SB} >}{\parallel \vec{SU} \parallel \parallel \vec{SB} \parallel}\right)$$

Where:

$$< \vec{SU}, \vec{SB} >= x_1x_2 + y_1y_2 + z_1z_2$$
$$\parallel \vec{SU} \parallel = \sqrt{x_1^2 + y_1^2 + z_1^2}$$
$$\parallel \vec{SB} \parallel = \sqrt{x_2^2 + y_2^2 + z_2^2}$$

First, we differentiate the dot product.

$$\frac{\partial <\vec{SU},\vec{SB}>}{\partial \phi_b} = \cancelto{0}{\frac{\partial x_1}{\partial \phi_b}}x_2 + x_1\frac{\partial x_2}{\partial \phi_b} + \cancelto{0}{\frac{\partial y_1}{\partial \phi_b}}y_2 + y_1\frac{\partial y_2}{\partial \phi_b} + \cancelto{0}{\frac{\partial z_1}{\partial \phi_b}}z_2 + z_1\frac{\partial z_2}{\partial \phi_b}$$

$$= x_1\frac{\partial x_2}{\partial \phi_b} + y_1\frac{\partial y_2}{\partial \phi_b} + z_1\frac{\partial z_2}{\partial \phi_b}$$

$$\frac{\partial <\vec{SU},\vec{SB}>}{\partial \theta_b} = \cancelto{0}{\frac{\partial x_1}{\partial \theta_b}}x_2 + x_1\frac{\partial x_2}{\partial \theta_b} + \cancelto{0}{\frac{\partial y_1}{\partial \theta_b}}y_2 + y_1\frac{\partial y_2}{\partial \theta_b} + \cancelto{0}{\frac{\partial z_1}{\partial \theta_b}}z_2 + z_1\frac{\partial z_2}{\partial \theta_b}$$

$$= x_1\frac{\partial x_2}{\partial \theta_b} + y_1\frac{\partial y_2}{\partial \theta_b} + z_1\frac{\partial z_2}{\partial \theta_b}$$

After that, we differentiate the norms of the vectors.

$$\frac{\partial \parallel \vec{SU} \parallel}{\partial \phi_b} = 0 = \frac{\partial \parallel \vec{SU} \parallel}{\partial \theta_b}$$

$$\begin{array}{l} \frac{\partial \|\vec{SB}\|}{\partial \phi_b} = \frac{x_2 \frac{\partial x_2}{\partial \phi_b} + y_2 \frac{\partial y_2}{\partial \phi_b} + z_2 \frac{\partial z_2}{\partial \phi_b}}{\|\vec{SB}\|} \\ \frac{\partial \|\vec{SB}\|}{\partial \theta_b} = \frac{x_2 \frac{\partial x_2}{\partial \theta_b} + y_2 \frac{\partial y_2}{\partial \theta_b} + z_2 \frac{\partial z_2}{\partial \theta_b}}{\|\vec{SB}\|} \end{array}$$

Now, the differentiation of $\cos(\alpha)$, which we will call Φ for simplicity.

$$\Phi = \frac{< \vec{SU}, \vec{SB} >}{\parallel \vec{SU} \parallel \parallel \vec{SB} \parallel}$$

$$\begin{array}{l} \frac{\partial \Phi}{\partial \phi_b} = \frac{1}{\|\vec{SU}\|} \frac{\frac{\partial < \vec{SU}, \vec{SB} >}{\partial \phi_b} \|\vec{SB}\| - < \vec{SU}, \vec{SB} > \frac{\partial \|\vec{SB}\|}{\partial \phi_b}}{\|\vec{SB}\|^2} \\ \frac{\partial \Phi}{\partial \theta_b} = \frac{1}{\|\vec{SU}\|} \frac{\frac{\partial < \vec{SU}, \vec{SB} >}{\partial \theta_b} \|\vec{SB}\| - < \vec{SU}, \vec{SB} > \frac{\partial \|\vec{SB}\|}{\partial \theta_b}}{\|\vec{SB}\|^2} \end{array}$$

Finally,

$$\begin{array}{l} \frac{\partial \alpha}{\partial \phi_b} = \frac{\partial \alpha}{\partial \Phi} \frac{\partial \Phi}{\partial \phi_b} = \frac{-1}{\sqrt{1-\Phi^2}} \frac{\partial \Phi}{\partial \phi_b} \\ \frac{\partial \alpha}{\partial \theta_b} = \frac{\partial \alpha}{\partial \Phi} \frac{\partial \Phi}{\partial \theta_b} = \frac{-1}{\sqrt{1-\Phi^2}} \frac{\partial \Phi}{\partial \theta_b} \end{array}$$

Of course, α is a function of the position of the beam, regardless of its shape. Therefore,

$$\frac{\partial \alpha}{\partial k_b} = 0$$

A.2. The derivatives of D

The aim of this section is to find the derivatives of D_b, being it the effective reflector diameter of the antenna of a beam b. In particular, lets assume we have the following two entities:

- A beam b with coordinates (latitude, longitude) = (ϕ_b, θ_b).
- A satellite s with ECEF coordinates (x, y, z) = (x_s, y_s, z_s).

We know, by Equation 5.3.3, that $D_b = \sqrt{\underbrace{\frac{10^{\frac{40-30\cdot(1-(cos(\text{scanningAngle}))}{10}}}{\eta}}_{A}} \cdot k_b$. θ in this subsection is defined as the scanning angle of the beam. Note the absence of subindex to difference it from the longitude coordinate of the beam, θ_b.

The process is remarkably similar to the previous section. Let's define the three main points:

$$\begin{aligned} O &= (0,0,0) \\ B &= R(cos(\phi_b)cos(\theta_b), cos(\phi_b)sin(\theta_b), sin(\phi_b)) \\ S &= (x_s, y_s, z_s) \end{aligned}$$

The vectors $\vec{SO}$ and $\vec{SB}$ (nadir vector and beam as seen from the satellite) are:

$$\vec{SO} = (\underbrace{-x_s}_{x_1}, \underbrace{-y_s}_{y_1}, \underbrace{-z_s}_{z_1})$$

$$\vec{SB} = (\underbrace{Rcos(\phi_b)cos(\theta_b) - x_s}_{x_2}, \underbrace{Rcos(\phi_b)sin(\theta_b) - y_s}_{y_2}, \underbrace{Rsin(\phi_b) - z_s}_{z_2})$$

And we rename the coordinates as:

$$\begin{aligned} \vec{SO} &= (x_1(\phi_b, \theta_b), y_1(\phi_b, \theta_b), z_1(\phi_b, \theta_b)) \\ \vec{SB} &= (x_2(\phi_b, \theta_b), y_2(\phi_b, \theta_b), z_2(\phi_b, \theta_b)) \end{aligned}$$

Note that, in fact, x_1, y_1 and z_1 are constant with respect to our variables (ϕ_b, θ_b).

The partial derivatives that will be needed are:

$$\begin{aligned} \frac{\partial x_1}{\partial \phi_b} &= 0 & \frac{\partial x_1}{\partial \theta_b} &= 0 \\ \frac{\partial y_1}{\partial \phi_b} &= 0 & \frac{\partial y_1}{\partial \theta_b} &= 0 \\ \frac{\partial z_1}{\partial \phi_b} &= 0 & \frac{\partial z_1}{\partial \theta_b} &= 0 \\ \frac{\partial x_2}{\partial \phi_b} &= -Rsin(\phi_b)cos(\theta_b) & \frac{\partial x_2}{\partial \theta_b} &= -Rcos(\phi_b)sin(\theta_b) \\ \frac{\partial y_2}{\partial \phi_b} &= -Rsin(\phi_b)sin(\theta_b) & \frac{\partial y_2}{\partial \theta_b} &= Rcos(\phi_b)cos(\theta_b) \\ \frac{\partial z_2}{\partial \phi_b} &= Rcos(\phi_b) & \frac{\partial z_2}{\partial \theta_b} &= 0 \end{aligned}$$

Using the dot product of these two vectors, we know that the angle θ between $\vec{SO}$ and $\vec{SB}$ is:

$$\theta = cos^{-1}\left(\frac{< \vec{SO}, \vec{SB} >}{\| \vec{SO} \| \| \vec{SB} \|}\right)$$

Where:

$$\begin{aligned} < \vec{SO}, \vec{SB} > &= x_1x_2 + y_1y_2 + z_1z_2 \\ \| \vec{SO} \| &= \sqrt{x_1^2 + y_1^2 + z_1^2} \\ \| \vec{SB} \| &= \sqrt{x_2^2 + y_2^2 + z_2^2} \end{aligned}$$

First, we differentiate the dot product.

$$\frac{\partial <\vec{SO},\vec{SB}>}{\partial \phi_b} = \cancelto{0}{\frac{\partial x_1}{\partial \phi_b}} x_2 + x_1 \frac{\partial x_2}{\partial \phi_b} + \cancelto{0}{\frac{\partial y_1}{\partial \phi_b}} y_2 + y_1 \frac{\partial y_2}{\partial \phi_b} + \cancelto{0}{\frac{\partial z_1}{\partial \phi_b}} z_2 + z_1 \frac{\partial z_2}{\partial \phi_b}$$

$$= x_1 \frac{\partial x_2}{\partial \phi_b} + y_1 \frac{\partial y_2}{\partial \phi_b} + z_1 \frac{\partial z_2}{\partial \phi_b}$$

$$\frac{\partial <\vec{SO},\vec{SB}>}{\partial \theta_b} = \cancelto{0}{\frac{\partial x_1}{\partial \theta_b}} x_2 + x_1 \frac{\partial x_2}{\partial \theta_b} + \cancelto{0}{\frac{\partial y_1}{\partial \theta_b}} y_2 + y_1 \frac{\partial y_2}{\partial \theta_b} + \cancelto{0}{\frac{\partial z_1}{\partial \theta_b}} z_2 + z_1 \frac{\partial z_2}{\partial \theta_b}$$

$$= x_1 \frac{\partial x_2}{\partial \theta_b} + y_1 \frac{\partial y_2}{\partial \theta_b} + z_1 \frac{\partial z_2}{\partial \theta_b}$$

After that, we differentiate the norms of the vectors.

$$\frac{\partial \parallel \vec{SO} \parallel}{\partial \phi_b} = 0 = \frac{\partial \parallel \vec{SO} \parallel}{\partial \theta_b}$$

$$\frac{\partial \|\vec{SB}\|}{\partial \phi_b} = \frac{x_2 \frac{\partial x_2}{\partial \phi_b} + y_2 \frac{\partial y_2}{\partial \phi_b} + z_2 \frac{\partial z_2}{\partial \phi_b}}{\|\vec{SB}\|}$$
$$\frac{\partial \|\vec{SB}\|}{\partial \theta_b} = \frac{x_2 \frac{\partial x_2}{\partial \theta_b} + y_2 \frac{\partial y_2}{\partial \theta_b} + z_2 \frac{\partial z_2}{\partial \theta_b}}{\|\vec{SB}\|}$$

Now, the differentiation of $\cos(\theta)$, which we will call Φ for simplicity.

$$\Phi = \frac{<\vec{SO}, \vec{SB}>}{\parallel \vec{SO} \parallel \parallel \vec{SB} \parallel}$$

$$\frac{\partial \Phi}{\partial \phi_b} = \frac{1}{\|\vec{SO}\|} \frac{\frac{\partial <\vec{SO},\vec{SB}>}{\partial \phi_b} \|\vec{SB}\| - <\vec{SO},\vec{SB}> \frac{\partial \|\vec{SB}\|}{\partial \phi_b}}{\|\vec{SB}\|^2}$$
$$\frac{\partial \Phi}{\partial \theta_b} = \frac{1}{\|\vec{SO}\|} \frac{\frac{\partial <\vec{SO},\vec{SB}>}{\partial \theta_b} \|\vec{SB}\| - <\vec{SO},\vec{SB}> \frac{\partial \|\vec{SB}\|}{\partial \theta_b}}{\|\vec{SB}\|^2}$$

Finally,

$$\frac{\partial D_b}{\partial \phi_b} = \frac{c}{\pi f} \frac{1}{2\sqrt{A}} \frac{1}{\eta} 10^{\frac{40-30\cdot(1-\Phi)}{10}} \frac{1}{10} 30 \frac{\partial \Phi}{\partial \phi_b} k_b$$

$$\frac{\partial D_b}{\partial \theta_b} = \frac{c}{\pi f} \frac{1}{2\sqrt{A}} \frac{1}{\eta} 10^{\frac{40-30\cdot(1-\Phi)}{10}} \frac{1}{10} 30 \frac{\partial \Phi}{\partial \theta_b} k_b$$

$$\frac{\partial D_b}{\partial k_b} = \frac{c}{\pi f} \sqrt{A}$$

A.3. The derivatives of a

Now we can compute the derivatives of a. We know that the value of this variable depends on D_b by the following relation:

$$a = \underbrace{-12 \frac{f^2}{70^2 c^2}}_{\text{const}} D_b^2$$

With the previous section, the derivatives of a become straightforward to compute.

$$\frac{\partial a}{\partial \phi_b} = 2 \text{ const } D_b \frac{\partial D_b}{\partial \phi_b}$$

$$\frac{\partial a}{\partial \theta_b} = 2 \text{ const } D_b \frac{\partial D_b}{\partial \theta_b}$$

$$\frac{\partial a}{\partial k_b} = 2 \text{ const } D_b \frac{\partial D_b}{\partial k_b}$$

A.4. The derivatives of b

Finally, we compute the derivatives of b. From Equations 5.3.4 and 5.3.5, we know the value of b as a function of k_b and the scanning angle.

$$b = 40 - 30 \cdot (1 - \Phi) + 20\log_{10}(k_b)$$

Were Φ is maintained, from other sections, as $cos(\theta)$.

$$\frac{\partial b}{\partial \phi_b} = 30 \frac{\partial \Phi}{\partial \phi_b}$$

$$\frac{\partial b}{\partial \theta_b} = 30 \frac{\partial \Phi}{\partial \theta_b}$$

$$\frac{\partial b}{\partial k_b} = \frac{20}{log(10)} \frac{1}{k_b}$$

Bibliography

[1] David Whitefield and Rajeev Gopal. Capacity enhancement with dynamic resource management for next generation satellite systems. *Military Communications Conference, 2005*, pages 761–767, 2005.

[2] Shiv Kumar Das. GPS, GIS and their uses, 2014.

[3] Gerard Maral and Michel Bousquet. *Satellite communications systems*. John Wiley & Sons, 5th edition, 2009.

[4] Nils Pachler, Markus Guerster, Inigo del Portillo, Edward F Crawley, and Bruce G Cameron. Static beam placement and frequency plan algorithms for LEO constellations. *International Journal of Satellite Communications and Networking (under review)*, 2020.

[5] Víctor Suárez-Paniagua. *Deep Learning for Information Extraction in the Biomedical Domain*. PhD thesis, 2019.

[6] *Satellite Communications*, 1997.

[7] SES S.A. SES NEW FRONTIERS Annual Report 2017. Technical report, 2017.

[8] Cédric Balty, Jean Didier Gayrard, and Patrick Agnieray. Communication satellites to enter a new age of flexibility. *Acta Astronautica*, 65(1-2):75–81, 2009.

[9] S E Holdings. LLC, SpaceX Ka-band NGSO constellation FCC filing SAT-LOA-20161115-00118, 2018.

[10] T Canada. Telesat Ka-band NGSO constellation FCC filing SAT-PDR-20161115-00108, 2018.

[11] W S Limited. "OneWeb Ka-band NGSO constellation FCC filing SAT-LOI-20160428-00041, 2018.

[12] Viasat. Going Global - Viasat-2 and the Viasat-3 Platform Will Take Our Service Around the World, 2018.

[13] SES. Exponentially More Opportunities With O3b mPOWER, 2018.

[14] Piero Angeletti, Riccardo De Gaudenzi, and Marco Lisi. From "bent pipes" to "software defined payloads": Evolution and trends of satellite communications systems. *26th AIAA International Communications Satellite Systems Conference, ICSSC*, pages 1–10, 2008.

[15] Markus Guerster, Juan Jose Garau Luis, Edward Crawley, and Bruce Cameron. Problem representation of dynamic resource allocation for flexible high throughput satellities. *IEEE Aerospace Conference Proceedings*, 2019-March, 2019.

[16] Inigo del Portillo. *Space and Aerial Architectures to Expand Global Connectivity*. PhD thesis, Massachusetts Institute of Technology, 2020.

[17] Jihwan P. Choi and Vincent W.S. Chan. Optimum power and beam allocation based on traffic demands and channel conditions over satellite downlinks. *IEEE Transactions on Wireless Communications*, 4(6):2983–2992, 2005.

[18] Jihwan P Choi and Vincent W S Chan. Optimum Multibeam Satellite Downlink Power Allocation Based on Traffic Demands. *Global Telecommunications Conference, 2002*, 3:2875–2881, 2002.

[19] Jihwan P. Choi and Vincent W.S. Chan. An efficient resource scheduling algorithm for phased array antenna satellites. *Proceedings - IEEE Military Communications Conference MILCOM*, 2006.

[20] Jihwan P. Choi and Vincent W.S. Chan. Resource management for advanced transmission antenna satellites. *IEEE Transactions on Wireless Communications*, 8(3):1308–1321, 2009.

[21] Axel Jahn. Resource management model and performance evaluation for satellite communications. *International Journal of Satellite Communications*, 19(2):169–203, 2001.

[22] Jean Thomas Camino, Christian Artigues, Laurent Houssin, and Stephane Mourgues. Mixed-integer linear programming for multibeam satellite systems design: Application to the beam layout optimization. *10th Annual International Systems Conference, SysCon 2016 - Proceedings*, 2016.

[23] Jean Thomas Camino, Stéphane Mourgues, Christian Artigues, and Laurent Houssin. A greedy approach combined with graph coloring for non-uniform beam layouts under antenna constraints in multibeam satellite systems. *2014 7th Advanced Satellite Multimedia Systems Conference and the 13th Signal Processing for Space Communications Workshop, ASMS/SPSC 2014*, 2014-Janua:374–381, 2014.

[24] Jean Thomas Camino, Christian Artigues, Laurent Houssin, and Stéphane Mourgues. Linearization of Euclidean norm dependent inequalities applied to multibeam satellites design. *Computational Optimization and Applications*, 73(2):679–705, 2019.

[25] Cen Qian, Sihai Zhang, and Wuyang Zhou. Traffic-based dynamic beam coverage adjustment in satellite mobile communication. *2014 6th International Conference on Wireless Communications and Signal Processing, WCSP 2014*, pages 1–6, 2014.

[26] Martin Schubert and Holger Boche. Solution of the multiuser downlink beamforming problem with individual SINR constraints. *IEEE Transactions on Vehicular Technology*, 53(1):18–28, 2004.

[27] Argyrios Kyrgiazos, Barry Evans, and Paul Thompson. Irregular beam sizes and non-uniform bandwidth allocation in HTS multibeam satellite systems. *31st AIAA International Communications Satellite Systems Conference, ICSSC 2013*, pages 1–8, 2013.

[28] Shree Krishna Sharma, Sina Maleki, Symeon Chatzinotas, Joel Grotz, Jens Krause, and Bjorn Ottersten. Joint Carrier Allocation and Beamforming for cognitive SatComs in Ka-band (17.3-18.1 GHz). *IEEE International Conference on Communications*, 2015-Septe:873–878, 2015.

[29] Bao Wenqian, Wang Weidong, Shuaijun Liu, and Cui Gaofeng. *Beam Coverage Dynamic Adjustment Scheme Based on Maximizing System Capacity for Multi-beam Satellite Communication System*, pages 288–298. 2018.

[30] Vahab Akbarzadeh, Julien Charles Lévesque, Christian Gagné, and Marc Parizeau. Efficient sensor placement optimization using gradient descent and probabilistic coverage. *Sensors (Switzerland)*, 14(8):15525–15552, 2014.

[31] ECC. The use of the frequency bands 27.5-30.0 GHz and 17.3-20.2 GHz by satellite networks. Technical report, 2010.

[32] International Telecommunication Union. SATELLITE SYSTEM CHARACTERISTICS TO BE CONSIDERED IN FREQUENCY SHARING ANALYSES BETWEEN GEOSTATIONARY-SATELLITE ORBIT (GSO) AND NON-GSO SATELLITE SYSTEMS IN THE FIXED-SATELLITE SERVICE (FSS) INCLUDING FEEDER LINKS FOR THE MOBILE-SATELLITE SERVICE (MSS). Technical report, 2005.

[33] Miguel Ángel Vázquez, Ana Pérez-Neira, Dimitrios Christopoulos, Symeon Chatzinotas, Björn Ottersten, Pantelis Daniel Arapoglou, Alberto Ginesi, and Giorgio Tarocco. Precoding in multibeam satellite communications: Present and future challenges. *IEEE Wireless Communications*, 23(6):88–95, 2016.